Journal of Drug Delivery Science and Technology 117 (2026) 107977

Contents lists available at ScienceDirect

Journal of Drug Delivery Science and Technology

journal homepage: www.elsevier.com/locate/jddst

Gunnera perpensa L. - mediated gold nanoparticles with enhanced anti-gonococcal activity

Tanyaradzwa Tiandra Dembetembe [a], Danielle Twilley [a], Jacqueline Maphutha [a], Marco Nuno De Canha [a], Velaphi Clement Thipe [b], Vusani Mandiwana [c], Michel Lonji Kalombo [c], Rirhandzu Rikhotso [c], Suprakas Sinha Ray [d], Namrita Lall [a,e,f], Quenton Kritzinger [a,*]

[a] Department of Plant and Soil Sciences, University of Pretoria, Pretoria, 0028, South Africa
[b] Department of Radiology, Institute of Green Nanotechnology, University of Missouri, Columbia, MO, 65212, United States
[c] Chemical Cluster, Centre for Nanostructures and Advanced Materials, Council for Scientific and Industrial Research, Pretoria, 0001, South Africa
[d] DST-CSIR National Centre for Nano-Structured Materials, Gauteng, Pretoria, 0001, South Africa
[e] School of Natural Resources, College of Agriculture, Food and Natural Resources, University of Missouri, Columbia, MO, 65211, United States
[f] College of Pharmacy, JSS Academy of Higher Education and Research, Mauritius

ARTICLE INFO

Keywords:
Gunnera perpensa L.
Gold nanoparticles
Sexually transmitted disease
Cytotoxicity
Gonorrhoea
Medicinal plants

ABSTRACT

Gonorrhoea is the second most prevalent sexually transmitted disease (STD) worldwide, with its treatment increasingly compromised by antibiotic resistance to available treatments. This has led to the investigation of bioactive plants as sources for novel drug development, with plant-based nanoparticles showing promise in treating STDs. This study aimed to evaluate the anti-gonococcal activity and cytotoxicity of the ethanolic root extract of *Gunnera perpensa* L. (GP) and to determine whether synthesis of gold nanoparticles (AuNPs) from GP showed enhanced biological activity. Characterization of the nanoparticles was performed using ultraviolet–visible spectrometry (UV–Vis), transmission electron microscopy (TEM), dynamic light scattering (DLS), Zeta potential, Fourier-transform infrared spectroscopy (FTIR) and X-ray diffraction (XRD). Lastly, the anti-gonococcal activity and cytotoxicity of GP and GP-AuNPs were evaluated. The AuNPs exhibited a surface plasmon resonance at 536 nm, confirming the successful synthesis of nanoparticles, with a hydrodynamic size of 127.20 nm and a core size of 39.51 nm. The GP-AuNPs showed enhanced anti-gonococcal activity compared to GP with a minimum inhibitory concentration (MIC) of 10.40 and 46.70 μg/mL, respectively. Cytotoxicity was evaluated on human keratinocytes (HaCaT), human monocytes (THP-1), and STD-related human cervical adenocarcinoma (HeLa), with GP-AuNPs exhibiting fifty percent inhibitory concentrations (IC_{50}) of 22.12 ± 0.52, 27.53 ± 6.02, and >38.96 μg/mL, respectively. In contrast, GP showed IC_{50} values > 400 μg/mL against all tested cell lines. These findings indicate that GP-AuNPs exhibit significant anti-gonococcal activity with greater selectivity for *Neisseria gonorrhoeae* over non-cancerous (HaCaT and THP-1) cells, as evidenced by selectivity indices (SIs) > 2. These findings suggest that both GP and GP-AuNP possess potential as lead candidates for the treatment of gonorrhoea. Their limited antiproliferative activity against HeLa cells (SI < 0.7) indicates they are unsuitable for treating STD-associated cervical cancers. To the best of our knowledge, no published studies have investigated the effect of plant-synthesized nanoparticles on their activity against *N. gonorrhoeae*; therefore, this is the first use of GP-AuNPs against *N. gonorrhoeae*, advancing plant-based nanomedicine for STDs.

1. Introduction

Gonorrhoea is a sexually transmitted disease (STD) with an estimated 82 million cases recorded each year globally, with Africa showing the highest incidence rate [1,2]. In 2016, it was estimated that there were ~22 million incidences of gonorrhoea reported in Africa [3]. In South Africa, gonorrhoea is the most prevalent bacterial STD, second to chlamydia, with 4.5 million active cases reported in 2017 [4].

* Corresponding author.
E-mail address: quenton.kritzinger@up.ac.za (Q. Kritzinger).

https://doi.org/10.1016/j.jddst.2026.107977
Received 7 August 2025; Received in revised form 9 December 2025; Accepted 1 January 2026
Available online 7 January 2026

Gonorrhoea is more prevalent in females, with studies in 2016 indicating that women accounted for 0.90 % of worldwide gonococcal cases compared to 0.70 % in males [3,5]. A 2017 study focusing on South African gonococcal infections reported that 6.60 % of the cases were attributed to females, while males accounted for 3.50 % [6]. The high incidence of infections and the emergence of multidrug-resistant strains make gonorrhoea a significant public health concern [7]. In South Africa, there have been reports of drug resistance to five major antibiotics: penicillin, tetracycline, cefixime, azithromycin, and ciprofloxacin [8].

Gonorrhoea is caused by *Neisseria gonorrhoeae,* a Gram-negative diplococcus bacterium that thrives in anoxic conditions and predominantly affects the genital mucosal membranes of humans [9,10]. This bacterium is highly infectious and has a heightened likelihood of reinfection due to its ability to evade the host immune system, promoting constitutive inflammation [11–13]. The persistence and high infection rates pose a significant threat to the efficacy of first-line drugs used to treat gonorrhoea, leading to the emergence of multidrug-resistant (MDR) and extensively drug-resistant (XDR) strains of *N. gonorrhoeae* [7,14,15]. Multidrug-resistant bacterial strains are defined as having resistance to at least one of the current recommended therapies and to at least two old antibiotic treatments, including penicillin, tetracycline, erythromycin, or ciprofloxacin. Strains with resistance to at least two of the current recommended therapies and resistance to no less than two of the old antibiotic treatments are categorized as XDR strains [7,16].

The surge in antibiotic resistance among gonococcal strains reduces the effectiveness of treatments, thereby increasing the persistence of the disease. Plants provide a source of potential novel drugs for the treatment of gonococcal infections including drug-resistant gonorrhoea. Ethnobotanical studies have shown that various plants are traditionally used worldwide to treat STDs and other diseases. Phytochemistry studies further show that plants exhibit rich chemical diversity and are therefore a valuable source for the development of novel anti-gonococcal and anti-STD therapeutics [17–21]. Several South African medicinal plants, such as *Aloe ferox* Mill. and *Peltophorum africanum* Sond., are traditionally used to treat gonorrhoea, with some of their isolated compounds (such as aloin) having anti-gonococcal activity [22–25].

Recently, nanotechnology has been explored to enhance drug bioavailability and drug load for the treatment of STDs, such as gonorrhoea [26,27]. Nanotechnology-based delivery systems can be incorporated into vaginal formulations as their nanoscale size facilitates passage through the vaginal barrier, termed the cervicovaginal mucus (CVM) [28–30]. The CVM only allows molecules less than 340 nm to pass through, indicating that nanoparticles below this threshold can be synthesized, potentially clear local and/or systemic gonococcal infections, as shown in Scheme 1 [28–30].

Several studies have reported nanoparticle-based formulations with anti-gonococcal activity; however, to the best of our knowledge, no published studies have investigated the effect of gold nanoparticles synthesized from plants on their activity against *N. gonorrhoeae*. A study by Lucío et al. [31] evaluated the effect of 5-mercapto-2-nitrobenzoic acid-coated silver nanoclusters (MNBA-AgNCs) against MDR *N. gonorrhoeae*. The MNBA-AgNCs showed significantly higher activity against *N. gonorrhoeae* than ceftriaxone and azithromycin, both in planktonic bacteria and in infected human conjunctival cells. Yang et al. [32] evaluated the activity of a tellurium-based compound, ammonium trichloro (dioxoethylene-O,O') tellurate, against two isolates of *N. gonorrhoeae*, with MIC values of 0.05 mg/mL against both MS11 and WHO isolates. The compound significantly decreased biofilm formation, continuous growth, and infectivity in endocervical (ME180) and colorectal (T84) endothelial cells. Alqahtani et al. [33] observed the effect of chitosan nanoparticles against thirteen different WHO strains of *N. gonorrhoeae* and against HeLa cells. The minimum inhibitory

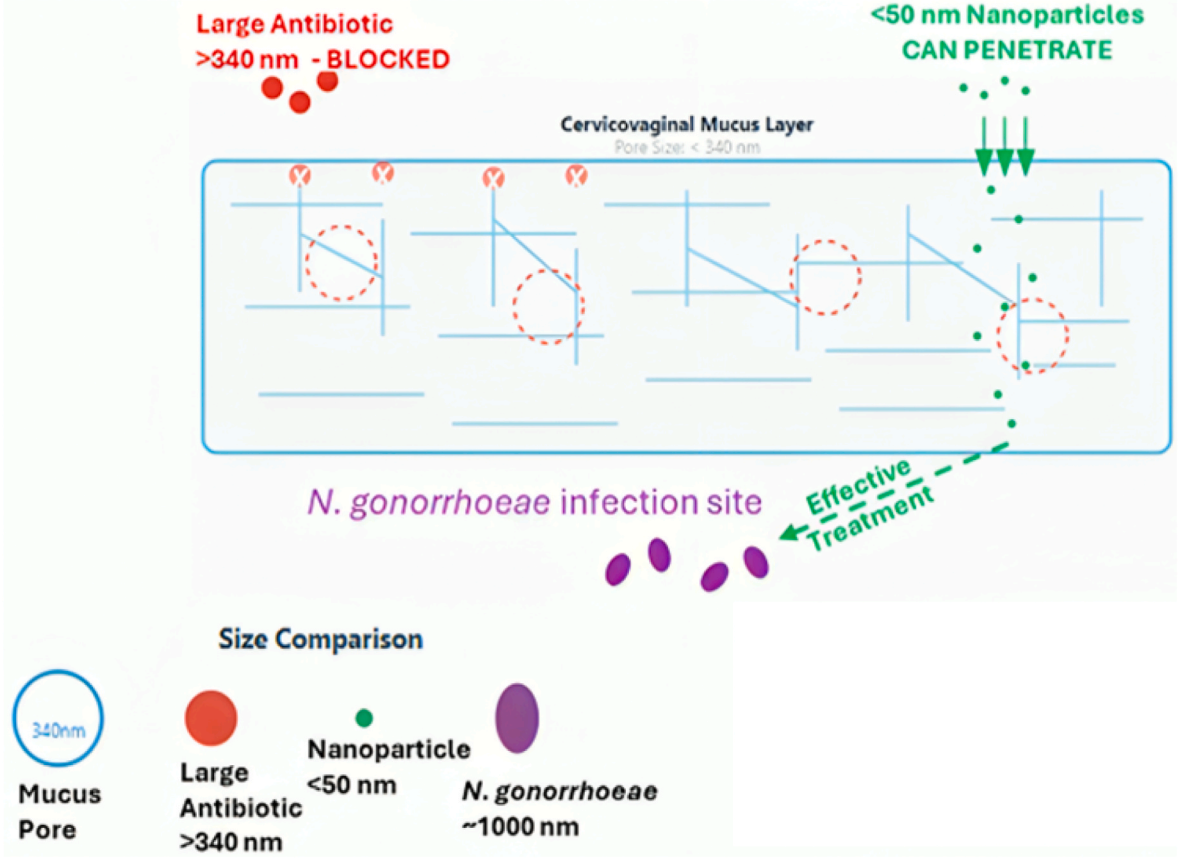

Scheme 1. Schematic of a nanoparticle-based strategy to combat *N. gonorrhoeae* with nanoparticles <50 nm that penetrate the cervicovaginal mucus layer (<340 nm pores), reaching the infection site and enabling localized, effective treatment of gonococcal infections.

concentrations (MICs) required to inhibit 90 % of growth ranged from 0.16 to 0.31 mg/mL, including MDR strains. Furthermore, the chitosan nanoparticles did not exhibit significant cytotoxicity against HeLa cells but did reduce bacterial adhesion to the cells. A study by Li et al. [34], showed that twenty-one different nanomaterials enhanced the activity of cefmetazole against MDR *N. gonorrhoeae*, including aluminium oxide, tin oxide, tungsten, silver, zinc oxide, iron oxide, titanium dioxide, and single- and multi-walled carbon nanotubes. The highest activity in reducing *N. gonorrhoeae* colony formation was observed in silver nanoparticles (120 nm) with an MIC of 12.5 μg/mL, whereas combining cefmetazole produced additive effects.

Inorganic nanoparticles prepared using silver and gold have been developed for the treatment of wounds, tuberculosis, cancer, and STDs [35–39]. The nanoparticles have the bioactive agent loaded onto the surface or encapsulated in the inorganic metal. These nanoparticles can be further capped with a stabilizer (such as gum arabic) to increase shelf-life [40,41]. Gold nanoparticles (AuNPs) are easily phagocytosed by cells and can deliver capped phytochemicals into bacterial cells [40, 42]. The green synthesis of AuNPs using bioactive compounds produced by plants, algae, fungi and microorganisms has gained notoriety, providing several advantages over chemical synthesis methods. Chemical synthesis of metal nanoparticles often requires high energy inputs, releases toxic chemicals, and requires specialised equipment to maintain synthesis conditions. Physical synthetic methods include aerosol-based methods and UV- and thermal-decomposition methods, which require substantial energy and increase production costs. Green nanoparticle synthesis requires low-energy experimental conditions (pH, temperature, and pressure) and non-toxic reducing and capping agents, making the process more cost-effective, environmentally safe, and less hazardous to human health. Metal nanoparticles synthesized by green techniques vary in size and shape, resulting in diverse physical, chemical, biological and biocompatibility properties [43,44].

Thipe et al. [40] demonstrated that resveratrol AuNPs (64 nm) can readily be phagocytosed by breast cancer (MDA-MB-231) and prostate cancer (PC-3) cells. Gold nanoparticles have predominantly been developed for the treatment of the human immunodeficiency virus (HIV) and herpes simplex virus (HSV) infections [40–43]. Baram-Pinto et al. [45] synthesized multivalent AuNPs mediated with mercaptoethane sulfonate, which affects viral entry and attachment of HSV-1. Di Gianvincenzo et al. [46] produced AuNPs with several sulfur ligands that can bind to the gp120 protein of HIV, thereby inhibiting infection. Nanoparticles have been employed to increase the bioavailability and efficacy of plant bioactive compounds. Plant-mediated AuNPs have been reported to have activity against STD pathogens [47,48]. *Sargassum wightii* Greville ex J. Agardh (brown algae) AuNPs have been found to inhibit the cytopathic effects of HSV-1 & 2 by 70 % at concentrations of 2.50 μL and 10 μL per sample, with no cytotoxic effects observed on Vero (African green monkey kidney epithelial) cells [49]. These findings indicate that AuNPs could potentially be used to treat STDs due to their ability to interfere with bacterial metabolic processes, damage bacterial DNA, disrupt bacterial membranes and inhibit microbial cell attachment [50,51].

Gunnera perpensa L., a member of the Gunneraceae family, is a South African medicinal plant commonly known as “wild rhubarb” or “river pumpkin” [23]. It is widely distributed throughout Africa, with occurrences across South Africa except in the Northern Cape [52,53]. The plant grows in waterlogged soils or near riversides [52,54]. Traditionally the rhizomes and roots are used to prepare decoctions that are administered orally to treat STDs (such as gonorrhoea and syphilis), stomach disorders, antenatal health problems, cancers, rheumatic fevers, dysmenorrhoea, wounds, psoriasis and urinary tract infections [23, 52,55–57].

The present study evaluated the anti-gonococcal activity and cytotoxicity of the ethanolic root extract of *Gunnera perpensa* L. (GP). Gold nanoparticles were synthesized using GP (GP-AuNPs) to determine whether the nanoparticles showed enhanced biological activity. Cytotoxic effects were evaluated on human keratinocytes (HaCaT) and human monocytes (THP-1), which represent non-cancerous cell lines; while the human cervical adenocarcinoma cell line (HeLa) was used to evaluate potential effects on STD-related cervical cancers. The GP-AuNPs were characterized using ultraviolet–visible spectrometry (UV–Vis), transmission electron microscopy (TEM), dynamic light scattering (DLS), Fourier-transform infrared spectroscopy (FTIR), Zeta potential and X-ray diffraction (XRD). This is the first use of GP-AuNPs against *N. gonorrhoeae*, advancing plant-based nanomedicine for STDs.

2. Materials and methods

2.1. Chemicals, reagents, cell lines and bacterial strain

Ethanol (98 %), gold salt ($HAuCl_4$), bovine serum albumin (BSA), cysteine (Cys), dimethyl sulfoxide (DMSO), sodium chloride (NaCl) and gum arabic were obtained from Sigma-Aldrich (St. Louis, MO, USA). Cell culture materials, phosphate-buffered saline (PBS), Dulbecco's Modified Eagle Medium (DMEM), Minimum Essential Media (MEM), Roswell Park Memorial Institute Medium (RPMI 1640), foetal bovine serum (FBS), trypsin/EDTA, amphotericin B and antibiotics (penicillin and streptomycin), *Neisseria gonorrhoeae* strain NCTC 8375 (ATCC 19424), GC chocolate agar, CO_2Gen (2.5 L) sachets and Mueller-Hinton (MH) broth were supplied by ThermoFisher Scientific (South Africa). The immortalized human monocytes (THP-1) were provided by Cellonex (South Africa), and the human keratinocytes (HaCaT) were donated by the Department of Human Biology, University of Cape Town (Cape Town, South Africa). The human cervical adenocarcinoma (HeLa) cell line was provided by the Department of Biochemistry, Genetics and Microbiology at the University of Pretoria (Pretoria, South Africa).

2.2. Plant collection and extraction

Shade-dried roots of *G. perpensa* were obtained from a commercial supplier, Muthi Futhi™, Uthungulu district, KwaZulu-Natal, South Africa. Plant extraction was conducted according to a method previously described Dembetembe et al. [58]. The plant material (400 g) was ground to a fine powder (Janke & Kunkel, MF 10, Germany) and macerated in absolute ethanol (2 L) with continuous shaking (Labcon 3086 U shaker, South Africa) at 140 rpm for 72 h. The extract was filtered under vacuum using a Büchner funnel with Whatman No. 1 filter paper. Subsequently, a vacuum rotary evaporator (Heidolph, Hei-Vap value digital HB/G3B, Germany) was used to remove excess solvent, yielding a concentrated extract, which was then air-dried in a fume hood to remove residual solvent. The extract was stored at 4 °C until further use.

2.3. Gold nanoparticle synthesis

The gold nanoparticles were synthesized using a method described by Thipe et al. [40], with minor modifications. Briefly, 60 mg of the ethanolic extract of *G. perpensa* (GP) was added to 30 mL of deionized water to prepare a stock concentration at 2 mg/mL. In a glass beaker, 46.70 mg of gum arabic (GA) was added to 14 mL of the GP stock solution, and the mixture was heated to 60 °C on a magnetic hot plate with continuous stirring at 700 rpm. Subsequently, 117 μL of 0.10 M gold salt ($HAuCl_4$) was added dropwise to the solution while stirring continuously for 30 min to synthesise GP-AuNPs. In addition, the same method was used to synthesise a second set of nanoparticles without gum arabic (GPX-AuNPs). Furthermore, a third set of AuNPs was synthesized (under the same conditions) using only GA, which served as a control to show that GA was not responsible for the reduction of gold salt. Nanoparticle formation was confirmed by the formation of a pink-red wine colour change, while a yellow solution without any precipitate was an indication of unsuccessful formation of AuNPs [59].

2.4. Characterization of nanoparticles

2.4.1. Ultraviolet–visible spectrometry

The surface plasmon resonance (SPR) was measured using UV–Vis spectrometry to confirm the formation of the nanoparticles according to a method described by De Canha et al. [60]. In a 96-well plate, 100 μL of GP-AuNPs and GPX-AuNPs, respectively, were added to the wells (in triplicate), and a full wavelength scan was performed from 200 to 800 nm (2 nm increments) at room temperature using a Victor Nivo multimode microplate reader (PerkinElmer, South Africa).

2.4.2. In vitro stability

The stability of the GP-AuNPs and GPX-AuNPs was determined using a method described by Thipe et al. [40], with modifications. The stability of the nanoparticles was evaluated using several buffer solutions of varying pH (pH 4, pH 7, pH 10) and several biological solutions (0.50 % Cys, 0.50 % NaCl, 0.50 % PBS, 0.50 % BSA, DMEM and deionized water [control]). Briefly, in separate Eppendorf tubes, the GP-AuNPs solution was added to each buffer solution at a 1:2 ratio, for a total volume of 1.5 mL. The same procedure was followed for the GPX-AuNPs. The Eppendorf tubes were incubated at 37 °C in 5 % CO_2 in a humidified incubator (Thermo Fisher Scientific, FormaTM 310, USA) for 24 h, 72 h, and 1 week. At each time interval, the SPR was determined by performing a full-wavelength scan from 200 to 800 nm (2 nm increments) using UV–Vis spectrometry.

2.4.3. Transmission Electron Microscopy (TEM)

Transmission electron microscopy (TEM) was used to determine the core size and shape of the synthesized GP-AuNPs, following the method described by De Canha et al. [60]. No further characterization was performed on GPX-AuNPs, as they were unstable in the abovementioned buffer solutions. The GP-AuNPs (5 μL) were loaded on a carbon-coated copper grid and dried overnight under a fume hood. A JEM-2100 transmission electron microscope (JEOL, Japan) equipped with X-MaxN 80T EDS was used to analyse the GP-AuNPs.

2.4.4. Dynamic Light Scattering (DLS) and zeta potential

The hydrodynamic size and surface charge (zeta potential) of the GP-AuNPs were determined using a Zetasizer Nano ZS (Malvern Panalytical Ltd, United Kingdom) according to the method described by De Canha et al. [60]. Eight hundred microliters (800 μL) of the freshly synthesized GP-AuNPs were dispensed into the DTS1070 folded capillary cell (Malvern Panalytical Ltd, United Kingdom) and placed in the Zetasizer Nano ZS (Malvern Instruments Ltd., Malvern, United Kingdom) at room temperature.

2.4.5. Fourier-transform infrared spectroscopy (FTIR)

Fourier-transform infrared spectroscopy was conducted following a method described by De Canha et al. [60]. The GP-AuNPs were freeze-dried, formed into a pellet, and placed in the sample holder. Surface conjugation and functional groups of the GP-AuNPs were determined using the PerkinElmer Spectrum 100 FTIR spectrophotometer (PerkinElmer, Midrand, South Africa). Measurements for percentage transmittance were obtained for the wavenumber range of 550–4000 cm^{-1}. The data was analysed using OriginPro software (OriginLab, version 2021).

2.4.6. X-Ray Diffraction (XRD)

The crystalline structure of the freeze-dried GP-AuNPs was determined by X-ray diffraction (XRD) using the PANalytical XPERT-PRO (Malvern Panalytical Ltd, United Kingdom) with a diffractometer using Ni-filtered CuK-α radiation (λ = 1.5406 Å) at 45kV/40 mA. The method described by De Canha et al. [60] was used to conduct XRD. The freeze-dried powder was ground into a fine powder and packed evenly into the sample holder. Data was analysed using OriginPro software. The crystalline size of GP-AuNPs was determined using Scherrer's law equation below:

$$D = \frac{k\lambda}{\beta \cos \theta}$$

where: D-crystallite size (nm), k- Scherrer constant = 0.90, λ-wavelength of the X-ray source, θ-peak position (radians), β-full width at half maximum (FWHM).

2.4.7. Quantification of total phenolic content

The Folin-Ciocalteu method was used to quantify the phenolic content of the GP-AuNPs as described by Thipe et al. [40]. Phenolics were quantified as they possess antimicrobial properties. The crude extract's phenolic content standard curve was generated to extrapolate the concentration of phenolics present in the GP-AuNPs. Briefly, 1 mL of GP (2 mg/mL in deionized water) was serially diluted (3.91–1000 μg/mL) in separate 5 mL Eppendorf tubes. Thereafter, 500 μL of 7.50 % sodium carbonate solution, mixed with 1 mL of 10 % Folin-Ciocalteu reagent, was added to each reaction tube, bringing the total volume to 2.5 mL. The final concentrations ranged from 1.56 to 400 μg/mL. In a separate 5 mL Eppendorf tube, 1 mL of the GP-AuNPs was added to the sodium carbonate solution and Folin-Ciocalteu reagent as mentioned above. All reaction tubes were incubated in a water bath at 30 °C for 30 min. After incubation, 100 μL of GP at each concentration and the GP-AuNPs were added to separate wells in a 96-well plate. Subsequently, absorbance was measured using a Victor Nivo multimode microplate reader at 760 nm. The phenolic content inferred from this assay was used to determine the test concentrations for the anti-gonococcal activity and cytotoxicity of the GP-AuNPs; therefore, the minimum inhibitory concentration (MIC) and 50 % inhibitory concentration (IC_{50}) values were reported as phenolic plant extract equivalents (PEE in μg/mL).

2.5. Preparation of inocula

Preparation of inocula was conducted according to the methods described by Tshikalange et al. [62] and Cos et al. [61]. Primary cultures of *N. gonorrhoeae* strain NCTC 8375 (ATCC 19424) were plated on GC chocolate agar at 37 °C for 48 h in a sealed container, with a 5 % CO_2 atmosphere maintained using CO_2Gen sachets. Subsequently, aliquots (1 mL) maintained in MH broth were collected into Eppendorf tubes and stored at −80 °C. Before the bioassays, inoculum suspensions were prepared by adding the contents of one aliquot to 50 mL of MH broth and incubating for 24 h at 37 °C in 5 % CO_2. To determine the amount of inoculum used for susceptibility testing, the bacterial suspensions were spectrophotometrically standardized to 0.5 McFarland and then adjusted to 1.50×10^5 colony-forming units (CFU)/mL.

2.6. Anti-gonococcal activity

The MIC of GP and the GP-AuNPs was determined using the microdilution assay described by Eloff [63]. A stock concentration of GP was prepared at 6 mg/mL in 10 % DMSO. In separate wells of a 96-well plate, 100 μL of GP and GP-AuNPs (in triplicate) were serially diluted two-fold (in MH broth) to obtain concentrations ranging from 23.40 to 3000 and 1.20 to 166.60 μg/mL, respectively. An inoculum of *N. gonorrhoeae* suspension was then added (100 μL) to obtain a final test concentration of 11.70–1500 μg/mL and 0.06–83.30 μg/mL for GP and GP-AuNPs, respectively. The plates were incubated at 37 °C for 24 h in 5 % CO_2. Ciprofloxacin (1 mg/mL in 10 % DMSO) was used as the positive control with a final concentration range of 1.95–250 μg/mL. Negative controls included a vehicle control with 10 % DMSO, a sterility control with MH broth (0 % growth) and a control with MH broth and the inoculum (100 % growth). The MIC was visually determined after the addition of 20 μL PrestoBlue (growth indicator) as described by Lall et al. [64]. A colour change from blue to pink indicated microbial growth.

2.7. Cell culture

Cells were cultured according to the method described by Lall et al. [64]. The HeLa cells were cultured in MEM, the HaCaT cells in DMEM, and the THP-1 cells in RPMI 1640. All relevant culture media used for cell culture were supplemented with 10 % FBS, 1 % antibiotics mixture (100 μg/mL penicillin and 100 μg/mL streptomycin) and 1 % antifungal agent (250 μg/mL amphotericin B). Cell lines were maintained in T75 culture flasks at 37 °C and 5 % CO_2 until confluent monolayers formed. Subsequently, cells were subcultured using 0.25 % trypsin/EDTA.

2.8. Cytotoxicity

The cytotoxicity potential of GP and GP-AuNPs was evaluated on HaCaT, THP-1 and HeLa cell lines according to the assay described by Lall et al. [64], using PrestoBlue as the cell viability agent. PrestoBlue is a blue, non-fluorescent resazurin-based indicator which reduces to resazurin, a pink fluorescent indicator formed in the presence of metabolically active cells Lall et al. [64]. The cells were seeded (1×10^5 cells/well) in 96-well plates (100 μL) using the respective media and grown in a humidified incubator at 37 °C in 5 % CO_2 for 24 h. Stock concentrations were prepared of GP (20 mg/mL in 2 % DMSO) and aqueous GP-AuNPs (332.86 μg/mL), followed by two-fold serial dilutions, which were added to the cells (in triplicate) to obtain final concentrations ranging from 3.125 to 400 μg/mL and 1.22 to 38.96 μg/mL, respectively. Actinomycin D (1 mg/mL) was used as the toxic inducer and tested at concentrations of 3.91×10^{-3} – 0.05 μg/mL. Additional controls included media control (without any cells; 0 %), vehicle control (2 % DMSO), and a negative control (cells in media; 100 %). The plates were incubated for 72 h at 37 °C in 5 % CO_2; thereafter, 20 μL of PrestoBlue was added to all wells, and the plates were incubated for a further 1 h. The fluorescence was measured at an excitation/emission of 560 nm/590 nm, respectively, using the Victor Nivo multimode plate reader. GraphPad Prism 7 (Version 7.04) software was used to calculate the IC_{50} values using the equation below.

$$\%\ Cell\ viability = \frac{FL.\ sample - FL.\ media\ control}{FL.\ vehicle\ control - FL.\ media\ control} \times 100$$

Where *FL.sample* – fluorescence of the sample, *FL.media control* – fluorescence of the media control (0 %), *FL.vehicle* – fluorescence of the vehicle control.

Furthermore, the selectivity index (SI) was calculated to evaluate the relation between (a) cytotoxicity on non-cancerous cell lines and antibacterial activity, and (b) cytotoxicity on non-cancerous and cancerous (HeLa) cell lines of GP and the AuNPs using the following equations:

a) $Selectivity\ index = \frac{IC50\ of\ non-cancerous\ cell\ cells}{MIC}$

b) $Selectivity\ index = \frac{IC50\ non-cancerous\ cells}{IC50\ of\ cancerous\ (HeLa)\ cells}$

2.9. Statistical analysis

All experimental data have been presented as mean ± standard deviation (SD) of three independent biological replicates (n = 3), with three technical replicates per experiment. To assess the statistical significance of the anti-gonococcal activity between the GP and GP-AuNPs, a Student's t-test was performed using GraphPad Prism 7.0. Statistical significance was evaluated using the *p*-value; $p < 0.05$ indicated a significant difference in antibacterial activity between treatments. For cytotoxicity, IC_{50} values were calculated by plotting log-transformed concentration (x-axis) against corresponding percentage viability (y-axis), followed by a non-linear regression curve fit (sigmoidal dose-response with variable slope) using GraphPad Prism 7.0 software.

3. Results and discussion

3.1. Synthesis, surface plasmon resonance and in vitro stability testing of GP-AuNPs and GPX-AuNPs

Two sets of gold nanoparticles were synthesized: GPX-AuNPs (without gum arabic) and GP-AuNPs (with gum arabic), whereas the gum arabic (GA) control (without plant extract) did not form AuNPs. The GA control was used to ensure that gum arabic did not contribute to AuNP synthesis and, therefore, was not responsible for the observed biological activity. The formation of red wine-coloured solutions of GPX-AuNPs and GP-AuNPs confirmed the synthesis of the NPs, which formed as a result of the reduction of gold ions (Au^{3+}) to zero-valent (Au^0), facilitated by the plant extract, resulting in the characteristic SPR of the synthesized AuNPs [59,65]. The SPR is an optical effect that results in a distinctive absorption peak in ultraviolet–visible spectrometry; thus, SPR can be used to confirm the formation of AuNPs. The SPR (λ_{max}) of GP-AuNPs and GPX-AuNPs were 536 nm and 542 nm, respectively (Fig. 1A), which were in the normal range of λ_{max} for AuNPs (530–545 nm) [40,60]. The GA control remained a yellow solution, indicating that the gold ions (Au3+) were not reduced, demonstrating that gum arabic contributed only to the stability of the AuNPs [66]. Thus, the GA control was not further characterized.

Gold nanoparticles synthesized from *Aspalathus linearis* (Burm.f.) R. Dahlgren and *Allium cepa* L. have been reported to both have λ_{max} of 535 nm [47,66]. De Canha et al. [60] synthesized *Helichrysum odoratissimum* L. Sweet AuNPs with λ_{max} of 540 nm, while Thipe et al. [40] developed AuNPs with resveratrol, a plant-derived compound, with λ_{max} of 535 nm. The SPR provides an indication of the shape and size of AuNPs, where narrower sharper peaks indicate monodispersed AuNPs of similar size and shape; hence, the GP-AuNPs were more monodispersed than the GPX-AuNPs, as they had a narrower λ_{max} peak [47,67,68]. Polydispersed nanoparticles are less bioactive than their monodispersed counterparts due to diversity in shape and size which promotes agglomeration [69,70].

The stability of the AuNPs was evaluated to determine whether they would agglomerate or flocculate over time under various conditions. Agglomeration increases the hydrophobicity of AuNPs, reducing their uptake into the bloodstream and interfering with their binding to enzyme active sites, thereby affecting the nanoparticles [47,68]. Furthermore, agglomeration alters the SPR, thereby affecting the optical properties of the AuNPs, leading to shifts in the SPR peaks [71,72]. The effects of the different buffer solutions, which mimic biological conditions, on the two sets of AuNPs after 24 h, 72 h and 1 week (Fig. 2A and B) showed that GPX-AuNPs were unstable compared to the GP-AuNPs, as GPX-AuNPs peaks became broader (exhibiting more horizontal shift) over time. The GPX-AuNPs showed the most significant SPR changes in 0.50 % NaCl after 24 h incubation, whereas they were unstable in 0.50 % cysteine and at pH 4 after a week. In these three buffer solutions (0.50 % NaCl, 0.50 % cysteine, pH 4), the GPX-AuNPs precipitated. This presents a significant challenge, as NaCl maintains osmotic pressure in the CVM, while the acidic pH (3.50–5.00) and elevated cysteine levels in the vagina prevent infections and support a healthy microbiota [73–76]. Conversely, the GP-AuNPs were moderately stable in all conditions for each time interval tested as the SPR peaks did not exhibit a horizontal shift or a change in peak intensity throughout. Furthermore, no agglomeration was observed in any buffer solution at any time interval. From these findings, the GP-AuNPs were more stable than the GPX-AuNPs due to the addition of gum arabic during synthesis; thus further characterization studies were performed on the GP-AuNPs.

Gum arabic is a non-toxic stabilizer used to cap the of the nanoparticles during synthesis, preventing agglomeration [40]. Previously, Thipe et al. [40] synthesized resveratrol AuNPs stabilized with gum arabic. These AuNPs had a stability profile similar to that of the GP-AuNPs in the present study. It has been shown that low pH

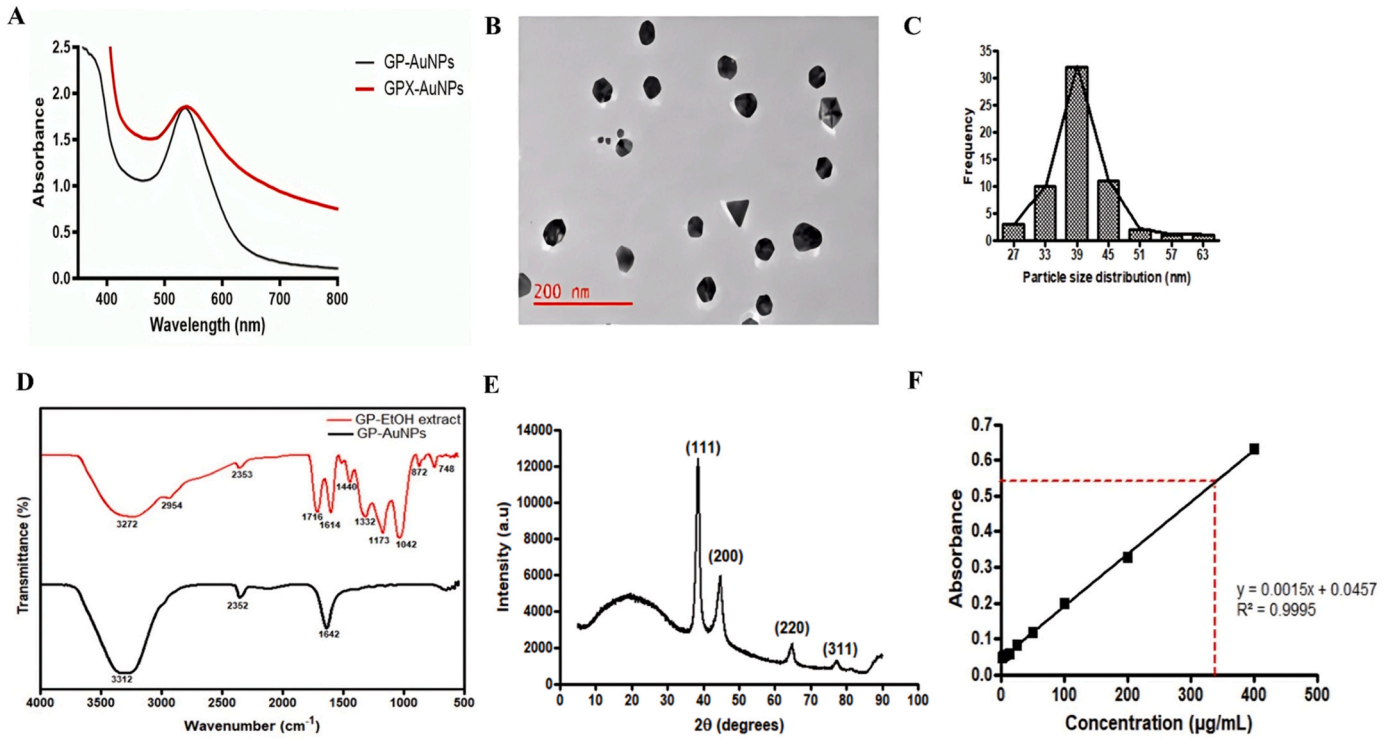

Fig. 1. **(A)** Surface plasmon resonance (SPR) of *Gunnera perpensa* gold nanoparticles synthesized with gum arabic (GP-AuNPs) and without gum arabic (GPX-AuNPs) obtained using ultraviolet–visible spectroscopy (UV–Vis), **(B)** Transmission electron microscopy (TEM) micrograph showing the morphology of the GP-AuNPs, **(C)** Particle size distribution of the GP-AuNPs using a Zeta-sizer **(D)** Fourier-Transform infrared spectra (FTIR) of *Gunnera perpens*a extract and GP-AuNPs, **(E)** X-ray diffraction pattern of GP-AuNPs using X-ray diffraction (XRD) and **(F)** *Gunnera perpensa* extract phenolic content standard curve. (For interpretation of the references to colour in this figure legend, the reader is referred to the Web version of this article.)

conditions and high salt environments reduce the stability of colloidal nanoparticles [77,78]. High NaCl concentrations decrease the Debye length of the AuNPs thus decreasing the repulsive forces between nanoparticles [79,80]. Debye length is the distance at which the separation between ions can occur [79,80]. Subsequently, there is an increase in the van der Waals forces between NPs, which reduces monodispersity and promotes agglomeration [77]. Capping polymers, such as gum arabic, maintain monodispersity by providing steric protection and preventing AuNPs from clumping [81–83].

3.2. Nanoparticle characterization

The GP-AuNPs were characterized using TEM, DLS, FTIR and XRD. The TEM analysis of the GP-AuNPs was used to determine the core size and shape of the nanoparticles. Most of the AuNPs were spherical, while a few were triangular and hexagonal (Fig. 1B). Furthermore, the average core size of the GP-AuNPs was 39.51 ± 6.46 nm (Fig. 1C). Blom van Staden et al. [66] synthesized gum arabic-stabilized *Aspalathus linearis* AuNPs that had the same morphology and a similar average core size of 39 nm.

The hydrodynamic size (Z-average) of GP-AuNPs was determined by DLS, yielding a Z-average of 127.20 ± 1.56 nm. The DLS was also used to determine the size distribution of the GP-AuNPs, which were relatively monodispersed, with a low polydispersity index (PDI) of 0.192. The polydispersity index is the measure of non-uniformity or heterogeneity of a sample. According to the International Organization for Standardization (ISO), highly monodispersed nanoparticles have PDI <0.05, while those with PDI >0.70 exhibit significant size variation [84,85]. For therapeutic action, nanoparticles with PDI <0.20 are acceptable, as variations in size promote agglomeration, which decreases the bioactivity of the AuNPs [70,84]. The hydrodynamic size of the GP-AuNPs (127.20 nm) was larger than the core size (39.51 nm) obtained from TEM. This is because the hydrodynamic size of AuNPs includes the nanoparticle core and the capping agents, which are attributed to the bioactive molecules in the *G. perpensa* extract and gum arabic. Furthermore, gum arabic is a high-molecular-weight polymer composed of glycoproteins and polysaccharides [86,87]. The highly branched nature of the molecule increases the hydrodynamic size of nanoparticles [40,86]. Likewise, Thipe et al. [40] synthesized gum arabic resveratrol AuNPs with a Z-average of 187.7 nm. The overall size of the GP-AuNPs makes them an ideal size (<340 nm) to pass the cervicovaginal mucus barrier of the vagina for the potential treatment of gonorrhoea in women [28,35,88].

The zeta potential of the GP-AuNPs was determined using dynamic light scattering. The zeta potential is the measure of surface charge on the nanoparticles, which indicates stability, where AuNPs with a zeta potential of > +30 mV and < −30 mV are considered strongly stable [89]. The GP-AuNPs exhibited a zeta potential of −5.34 ± 0.25 mV; however, the GP-AuNPs did not show any agglomeration. The absence of agglomeration in the GP-AuNPs may be attributed to the gum arabic stabilizer, which is known to increase the size of nanoparticles and provide steric protection, thereby enhancing stability [90,91]. Future studies could coat the nanoparticles with polyethene glycol (PEG) to increase the number of free thiols on the surface of the GP-AuNPs. This increases the surface negative charge, further enhancing the stability of the GP-AuNPs [92,93].

The characterization of functional groups in GP, which were potentially involved in reducing gold to synthesise GP-AuNPs, was evaluated using FTIR. The FTIR spectrum showed three distinct peaks at 3312 cm^{-1}, 2352 cm^{-1} and 1642 cm^{-1} in GP and GP-AuNPs (Fig. 1D). The peaks at 3312 cm^{-1} are characteristic of the hydrogen-bonded -OH functional group found in phenolic compounds such as venusol and punicalin, previously isolated from *G. perpensa* [90,91,94,95]. Punicalin has previously demonstrated antibacterial activity against *Streptococcus*

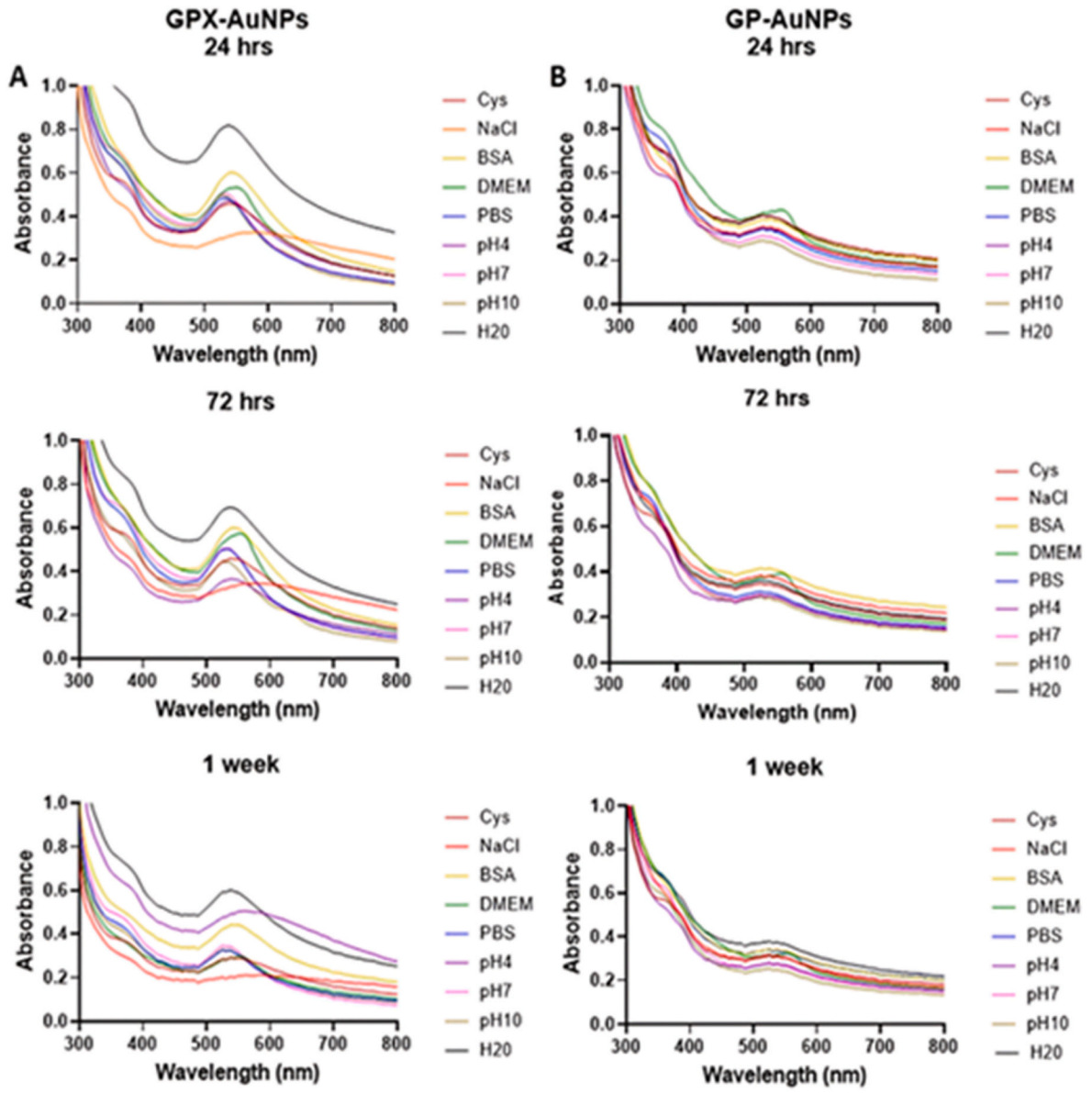

Fig. 2. *In vitro* stability of *Gunnera perpensa* gold nanoparticles synthesized with gum arabic **(A)** GPX-AuNPs and without gum arabic **(B)** GP-AuNPs in different biological media after 24 h, 72 h and 1 week. (For interpretation of the references to colour in this figure legend, the reader is referred to the Web version of this article.)

gordonii, *Streptococcus mutans* and *Streptococcus sobrinus*, with MIC values ranging between 100 and 200 μg/mL [96]. The peak at 2352 cm^{-1} indicates amino groups (-NH) interacting with the gold surface of the GP-AuNPs, which could be attributed to alkaloids present in the plant [91,97,98]. The peak at 1642 cm^{-1}, in the double bond region of the FTIR spectrum, correlates to a carbonyl group (C=O) in ketone compounds such as the 1,4 benzoquinones, 2-methyl-6-(-3-methyl-2-butenyl) benzo-1,4-quinone and 3-hydroxy-2-methyl-5-(3-methyl-2-butenyl) benzo-1,4-quinone present in *G. perpensa* [90,91,99]. The compound, 2-methyl-6-(-3-methyl-2-butenyl) benzo-1,4-quinone, has previously shown antibacterial activity against *Enterococcus faecalis* and *Staphylococcus aureus* with MIC values of 39 μg/mL, *Bacillus cereus* (MIC: 2.5 μg/mL) and *Staphylococcus epidermidis* with an MIC of 1.25 μg/mL [99]. These compounds have not been previously reported for their anti-gonococcal activity and should therefore be evaluated against *N. gonorrhoeae* to identify potential bioactive compounds in *G. perpensa*. Patel et al. [48] reported similar results, identifying the same functional groups as major components involved in the capping of *G. perpensa* during the synthesis of silver nanoparticles. The FTIR spectra of the ethanolic extract of *G. perpensa* and the GP-AuNPs were different (Fig. 1D), with GP having more peaks, in the 500-1700 cm^{-1} region, than the GP-AuNPs. This was because not all functional groups of the compounds in GP were involved in capping GP-AuNPs.

To determine the crystalline nature of the GP-AuNPs, XRD was used as shown in Fig. 1E. Four distinct peaks at 38.58°, 44.80°, 64.53° and 76.98° were observed with planes indexed at (111), (200), (220) and (311), respectively. These diffraction indices were consistent with cubic face-centred (FCC) gold particles according to the RRUFF database of Raman spectra and Joint Committee Powder Diffraction Standards USA [100], confirming the synthesis of the gold nanoparticles using *G. perpensa*. The same FCC indices have been recorded in onion peel AuNPs [47]. Additionally, the crystalline size of the GP-AuNPs and *d*-spacing (interplanar spacing) between crystals were determined (Table 1). Most of the crystals were ~6.41 nm, corresponding to the highest peak in Fig. 1E. The average *d*-spacing between two GP-AuNPs crystals in parallel planes in a lattice was ~2.34 nm.

Table 1
Crystallite size of GP-AuNPs and d-spacing between the crystals.

Peak position (2θ)	Crystallite size (nm)	*d*-spacing (nm)[a]
38.58	6.41	2.34
44.80	4.12	2.03
64.53	3.16	1.44
73.98	0.11	1.28

[a] Distance between crystals in parallel planes of the gold nanoparticles.

3.3. Phenolic quantification of GP-AuNPs

The phenolic content was measured as phenolics were one of the major classes in the crude plant extract which reduced the gold, as depicted in the FTIR spectra. Additionally, this group of compounds have been attributed to the observed antimicrobial and antioxidant activity of *G. perpensa* [52,101]. The phenolic content of the GP-AuNPs was extrapolated from the standard curve of GP (Fig. 1F). The GP-AuNPs had 332.86 μg/mL of phenolics as calculated using the equation $y = 0.0015x + 0.0457$. This was then used to determine the test concentrations for the antimicrobial susceptibility and cytotoxicity assays, and to determine the MIC and IC_{50} values.

3.4. Anti-gonococcal activity against Neisseria gonorrhoeae

The anti-gonococcal activity of GP and GP-AuNPs showed MIC values of 46.70 and 10.40 μg/mL, respectively (Table 2). Notably, GP-AuNPs exhibited significantly enhanced anti-gonococcal activity compared to GP alone ($p < 0.05$). *Gunnera perpensa* has not previously been evaluated against *N. gonorrhoeae*, despite its traditional use in the treatment of gonorrhoea; however, it has been reported for its activity against *Candida albicans*, an opportunistic STD pathogen (MIC: 6.25 mg/mL) [56]. *Gunnera perpensa* has also exhibited antibacterial and antifungal activity against other non-STD microbes such as *Staphylococcus aureus*, *Pseudomonas aeruginosa* and *Cutibacterium acnes* [102,103].

The observed results are consistent with previous reports showing that functionalized AuNPs with plant extracts exhibit enhanced antibacterial activity. Hussein et al. [104] demonstrated enhanced activity of an aqueous seed: peel (3:1) extract of *Punica granatum* (PE) against methicillin-resistant *Staphylococcus aureus* (MRSA). The extract alone had an MIC of 500 μg/mL, whereas the PE-AuNPs had an MIC of 125 μg/mL (4-fold increase in bioactivity). This activity was further enhanced when using chitosan-PE conjugated AuNPs (CS-PE-AuNPs), which showed an MIC of 15.6 μg/mL. The minimum bactericidal concentrations (MBC) also improved with PE, PE-AuNPs, and CS-PE-AuNPs, showing MBC values of >500, 500, and 62.5 μg/mL, respectively. While the specific mechanism of action of GP-AuNPs against *N. gonorrhoeae* was not investigated in this study, the significant anti-gonococcal activity observed may be attributed to previously described mechanisms by which gold nanoparticles (AuNPs) exert antibacterial effects. Gold nanoparticles have been reported to disrupt bacterial cell walls by inducing the production of reactive oxygen species (ROS) and interfering with essential metabolic processes [50,105,106]. Elevated ROS levels can damage bacterial membranes, inhibit adenosine triphosphate (ATP) synthesis, and disrupt overall cellular metabolism [107]. Furthermore, AuNPs are known to form strong interactions with the nitrogen, oxygen, and sulfur atoms of bacterial molecules, thereby providing broad-spectrum activity by altering bacterial membrane permeability [50,51,105,108]. These interactions can also cause DNA damage and inhibit critical bacterial enzymes, ultimately resulting in cell death [51,107].

There have been no previous reports on the activity of *G. perpensa* AuNPs against *N. gonorrhoeae*; however, auranofin, an orally administered, FDA-approved, gold-containing analogue used for rheumatoid arthritis, has been repurposed for its antibacterial activity against multidrug-resistant *N. gonorrhoeae*, exhibiting an MIC_{50} and MIC_{90} of 0.06 and 0.125 μg/mL, respectively. Previous studies have reported the potent antibacterial activity against clinically important pathogens, including multidrug-resistant *Staphylococcus aureus* (MRSA), vancomycin-resistant *enterococci* (VRE), and *Clostridioides difficile*. The FDA-approved status of auranofin highlights the potential of gold-containing therapeutic agents in addressing bacterial infections [109]. Lagha et al. [110] evaluated the antibacterial activity of polyvinyl-pyrrolidone (PVP) AuNPs against *N. gonorrhoeae* (ATCC 49226), reporting an MIC of 100 μg/mL and an MBC of 400 μg/mL.

Compared with ciprofloxacin, the positive control, which demonstrated an MIC <1.95 μg/mL, GP-AuNPs showed lower potency. Previous studies have reported an MIC <10 μg/mL for ciprofloxacin on the *N. gonorrhoeae* (ATCC 19424) strain, whilst some clinical isolates have been found to have MIC values ranging from 0.06 to 0.50 μg/mL [111,112]. Current first-line treatments for gonorrhoea include azithromycin, ceftriaxone and ciprofloxacin [16]. Azithromycin typically exhibits an MIC of <1 μg/mL for sensitive strains and ≥1 μg/mL for resistant strains. For ceftriaxone and ciprofloxacin, the thresholds are <0.06 μg/mL for sensitive strains and ≥1 μg/mL for ciprofloxacin and ≥0.25 μg/mL for ceftriaxone, respectively, for resistant strains [113]. Despite the GP-AuNPs exhibiting a 10-fold decrease in antibacterial potency compared to antibiotic standards, there are several advantages to using nanoparticles as drug delivery systems for antimicrobial agents. Due to their size, nanoparticles are biocompatible with the biomolecular

Table 2
Anti-gonococcal activity and cytotoxicity of the ethanolic root extract of *Gunnera perpensa* (GP) and *G. perpensa* gold nanoparticles (GP-AuNPs).

Samples	MIC[a] (μg/mL)	Cytotoxicity[‡] IC_{50}[b] ± SD[c] (μg/mL)			Selectivity index (SI)			
					Non-cancerous cell lines vs cancerous (HeLa) cells		Non-cancerous cell lines vs gonococcal cells	
		HeLa	HaCat	THP-1	HaCat	THP-1	HaCat	THP-1
***Gunnera perpensa* extract**	46.70	>400	>400	>400	–	–	>8.20	>8.20
GP-AuNPs[d]	**10.40**†	>38.96	22.12 ± 0.52	27.53 ± 6.02	<0.57	<0.71	2.13	2.64
Actinomycin D[e]	–	$2.11 \times 10^{-3} \pm 5.50 \times 10^{-4}$	$1.91 \times 10^{-3} \pm 4.58 \times 10^{-4}$	$8.44 \times 10^{-2} \pm 6.8 \times 10^{-3}$	–	–	–	–
Ciprofloxacin[f]	<1.95	–	–	–	–	–	–	–

- Not applicable.
†*p-value* < 0.05 for anti-gonococcal MIC when comparing GP to GP-AuNPs using a Student's t-test.
[a] Minimum inhibitory concentration.
[b] Fifty percent inhibitory concentration.
[c] Standard deviation.
[d] *Gunnera* perpensa gold nanoparticles (with gum arabic).
[e] Positive control for the cytotoxicity assay.
[f] Positive control for the anti-gonococcal activity.

structures of bacterial cells, enabling stronger interactions than small-molecule antibiotics. Nanoparticles have a high surface-to-volume ratio, which allows for a multitude of functionalized surface ligands to target bacteria [114]. A study by Lucío et al. [31] investigated the bactericidal activity of 5-mercapto-2-nitrobenzoic acid-coated silver nanoparticles (MNBA-AgNCs) against *N. gonorrhoeae*. The MNBA-AgNCs showed 50 % and 100 % bactericidal effects after 1 h of exposure to 0.019 μM and 0.467 μM, respectively. Lower doses of 0.001 μM and 0.005 μM showed bactericidal effects after 3 h of treatment. Ceftriaxone exhibited significantly lower potency, requiring 2.34 μM for 50 % bactericidal effects after 1 h of exposure and 0.467 μM after 3 h of exposure. The highest tested concentration of ceftriaxone, 11.7 μM, did not achieve 100 % bactericidal activity even after 3 h of exposure. Gürbay et al. [115] reported the toxicity of ciprofloxacin on isolated primary dermal fibroblasts after 24, 48 and 78 h of exposure. After 24 h, cell viability remained the same as the control; however, ciprofloxacin showed toxicity at 0.129 mM (42.75 μg/mL) and 0.194 mM (64.28 μg/mL) after 48 and 72 h of exposure, suggesting that long-term exposure to antibiotic treatments may have toxic effects. Rizvi et al. [116] describe factors that influence cytotoxic and pharmacological profiles of gold nanoparticles, namely, size, shape, surface chemistry and charge. Further investigation of the specific ligand-binding of *G. perpensa* antibacterial markers should be explored to determine whether specific ligands can enhance antibacterial activity. Furthermore, Ribeiro et al. [117] report methods for synthesizing AuNPs and mixing them with antibiotics to potentiate antibacterial activity. This is likely due to the unique interactions of gold nanoparticles with bacterial cell wall structures, which enhance the activity of antibiotic treatments and should also be considered. Furthermore, longer-term infection models using human epithelial cells should be considered, as demonstrated by Lucío et al. [31] and Yang et al. [32]. Prolonged infection with *N. gonorrhoeae* results in the formation of multiaggregate biofilm-like bacterial colonies on cell surfaces, decreasing the efficacy of antimicrobials [118,119].

Other metallic nanoparticle delivery systems, including silver (Ag) NPs, have also been investigated for antibacterial activity. Synthesized AgNPs from the methanolic extracts of *G. perpensa* on non-STD bacteria *Escherichia coli* (P4055) and *S. aureus* (S5878) both with MICs of 6.30 μg/mL, while AgNPs prepared from the aqueous extract had MICs of 3.20 μg/mL against both bacteria [48]. There have been several other reports on the activity of plant-based AuNPs against other STD pathogens. Dhanasezhian et al. [49] synthesized seaweed (*Sargassum wightii* Greville ex J. Agardh) AuNPs that exhibited antiviral activity against the herpes virus HSV-1. Folorunso et al. [120] produced *Annona muricata* L. AuNPs, which showed a 42 % inhibition at 4 μg/mL against *C. albicans*. Numerous AuNPs have been synthesized for the treatment of HIV using antiviral drugs [37,121–123]. Other plant-based AuNPs have been synthesized against non-STD pathogens such as *Staphylococcus epidermidis*, *E. coli, P. aeruginosa* and *S. aureus* with zones of inhibition ranging from 24 to 31 mm [124–126]. Furthermore, previous studies have reported the successful synthesis of plant-based nanoparticles using silver and organic polymers to treat non-STD ailments. Diedericks et al. [127] developed polymeric nanoparticles, using compounds isolated from plants, that exhibited anti-tuberculosis properties, while Keskin et al. [107] developed AgNPs from *Anchusa officinalis* that had antimicrobial effects against non-STD pathogens. Montazersaheb et al. [39] developed AgNPs using pumpkin to treat breast cancer. These findings highlight the pharmacological relevance of nanoparticles and support the rationale for the current study, which aims to develop plant-based treatments for gonorrhoea.

3.5. Cytotoxicity on non-cancerous and cancerous cell lines

Kuete and Efferth [108] describe cytotoxicity ranges for non-cancerous cell lines as follows: $IC_{50} > 400$ μg/mL (non-cytotoxic), $120 < IC_{50} < 400$ μg/mL (low cytotoxicity), $40 < IC_{50} < 120$ μg/mL (moderate cytotoxicity) and $IC_{50} < 40$ μg/mL (significantly cytotoxic). For cancerous cell lines, cytotoxicity thresholds are denoted as $IC_{50} > 100$ μg/mL (non-cytotoxic), $20 < IC_{50} < 100$ μg/mL (low cytotoxicity), $4 < IC_{50} < 20$ μg/mL (moderate cytotoxicity), and $IC_{50} < 4$ μg/mL (significantly cytotoxic). The cytotoxic effects of GP and GP-AuNPs were evaluated against non-cancerous HaCaT and THP-1 and cancerous HeLa cell lines. The HeLa cell line has been used in several studies as a suitable model for STDs. Xiao et al. [128] evaluated the expression of human papillomavirus (HPV) in HeLa cells; Sun et al. [129] studied *Chlamydia trachomatis* expression in the same cell line; and Heydarian et al. [130] highlighted the widespread use of HeLa cells as an epithelial model in many *N. gonorrhoeae* studies.

The GP extract showed no cytotoxicity against any of the tested cell lines, with IC_{50} values > 400 μg/mL (Table 2). Conversely, the GP-AuNPs were found to be cytotoxic to non-cancerous HaCaT and THP-1 cell lines, with IC_{50} values of 22.12 ± 0.52 and 27.53 ± 6.02 μg/mL, respectively. The GP-AuNPs exhibited low cytotoxicity against cancerous HeLa cells, with an IC_{50} above the highest tested concentration of 38.96 μg/mL. In contrast, positive control (toxic inducer), Actinomycin D, displayed IC_{50} values of $<8.44 \times 10^{-2}$ μg/mL against the tested cell lines.

The cytotoxicity of GP compares with previous studies. Lall et al. [103] report that the leaf ethanolic extracts of *G. perpensa* had no cytotoxicity to HaCaT cells ($IC_{50} > 400$ μg/mL). Several studies have shown that *G. perpensa* does not exhibit significant cytotoxic effects on non-cancerous cell lines [131,132]. Aqueous root extracts of *G. perpensa* have been found not to show substantial toxicity to murine macrophages (RAW 264.7) and human embryonic kidney cells (HEK 293) with IC_{50} values > 200 μg/mL [133,134]. Additionally, a methanolic root extract of *G. perpensa* was not cytotoxic to human fibroblast (MRC5) cells, with an $IC_{50} > 1000$ μg/mL [135].

There are no previous reports of the cytotoxicity of GP-AuNPs; however, the cytotoxic effects of silver nanoparticles (AgNPs) of *G. perpensa* have been reported by Lediga et al. [136]. The AgNPs prepared using the aqueous root extract of *G. perpensa* exhibited a >50 % mortality rate using the Brine Shrimp Lethality Assay. Other studies have elucidated the cytotoxicity of plant-mediated AuNPs in cancerous and non-cancerous cell lines. Blom van Staden et al. [66] reported that *Aspalathus linearis* AuNPs exhibited an IC_{50} of 67.51 μg/mL on normal human melanocytes (NHM), while Josiah et al. [135] evaluated the effects of cannabidiol AuNPs on HaCaT cells, exhibiting an IC_{50} of 23.99 μg/mL. On the other hand, Thipe et al. [40] reported that resveratrol AuNPs exhibited IC_{50} values of 72 μg/mL and 59 μg/mL on cancerous MDA-MB-231 and PC-3 cells, respectively. A study by Matić et al. [137] evaluated the cytotoxicity of luteolin-loaded gold nanoparticles against non-cancerous HaCaT cells and cancerous HeLa cells, with IC_{50} values of 48.39 ± 1.25 μg/mL and 9.21 ± 0.27 μg/mL, respectively. These studies suggest that nanoparticles synthesized from single, isolated compounds may exhibit greater specificity for cancerous cells than for non-cancerous cells, and that AuNPs synthesized from biomarker compounds from *G. perpensa* should be investigated for anti-gonococcal activity and cytotoxicity against STD-relevant HeLa cells.

The selective index (SI), representing the ratio of cytotoxicity of GP and GP-AuNPs against non-cancerous cell lines to that against bacterial cells, was >8 and > 2, respectively (Table 2). According to the guidelines of Kudumela et al. [138], Both samples showed selectivity for *N. gonorrhoeae* compared to non-cancerous cells, with SI > 1. Furthermore, the SI of the GP-AuNPs was calculated to compare the cytotoxicity ratios in non-cancerous cell lines to those in cancerous HeLa cells. This was done because the AuNPs showed greater cytotoxicity than GP. The GP-AuNPs exhibited selective indices <0.70 indicating that the GP-AuNPs were more cytotoxic to non-cancerous cells compared to the HeLa cells. Consequently, GP-AuNPs showed higher activity against *N. gonorrhoeae* than against non-cancerous cells; therefore, they may be an ideal candidate for further evaluation as a treatment for gonorrhoea. However, the GP-AuNPs may not be suitable as an anti-cancer treatment due to their low antiproliferative effects against cervical

adenocarcinoma cells. To date, no *in vitro* studies have investigated the cytotoxicity of GP and GP-AuNPs on HeLa and THP-1 cells.

Based on the findings of this study, GP-AuNPs exhibit a significant (4-fold increase) in anti-gonococcal activity compared to GP. Furthermore, the GP-AuNPs showed greater selectivity (SI $>$ 2) towards the bacteria compared to the non-cancerous cell lines. This provides scientific evidence that GP-AuNPs are promising candidates for further exploration as an anti-gonococcal therapy. However, their weak antiproliferative activity against the cancerous HeLa cells suggests that they may not be the preferred therapeutic agent for STD-induced cervical cancer. Longer-term cellular toxicity effects should be evaluated to determine whether they can induce apoptosis, DNA fragmentation, and caspase-3 and -8 activation with increased exposure times [139].

3.6. Limitations of the study

Despite the enhanced antibacterial activity of GP-AuNPs, several limitations of this study were identified. Evaluation of the antibacterial mechanism of action is required to elucidate the effects of GP-AuNPs on bacterial cell structures. In particular, the effects on *N. gonorrhoeae* resistance mechanisms need to be investigated to support their clinical relevance. For example, Mulaudzi et al. [140] demonstrated, *in silico* and *in vitro*, that *Helichrysum populifolium* DC. compounds inhibit the MtrCDE efflux pump, which contributes to antibiotic resistance, using the bis-benzimide accumulation assay. Lagha et al. [110] reported that plasmonic gold nanoprisms (PlAuNPR) inhibited *N. gonorrhoeae* biofilms. Additionally, Tseng et al. [141] highlighted how *N. gonorrhoeae* uses manganese (Mn^{2+}) as a non-antioxidant defence against superoxide anion ($O2^{-}$), which is produced during neutrophil attack. It was shown that a manganese transport protein C (MntC) mutant of *N. gonorrhoeae*, defective in the manganese ATP-binding cassette transporter, consisting of the ATP-binding component MntA, the permease MntB and the substrate binding protein MntC (MntABC) system, accumulated less Mn^{2+} and was sensitive to reactive oxygen species (ROS), suggesting that the manganese pathway is a potential target for inhibiting the bacterium. Taken together, GP and GP-AuNPs should be investigated in a similar manner to elucidate the mechanisms underlying their enhanced anti-gonococcal activity. Mechanistic studies assessing ROS generation and virulence factor expression could provide insight into how GP-AuNPs disrupt bacterial growth, biofilm formation, and anaerobic respiration. Opacity-associated (Opa) proteins, which are integral to bacterial adhesion and immune evasion, may yield further mechanistic insights [142,143]. Furthermore, GP and GP-AuNPs could be investigated against the nitrite reductase enzyme (AniA), which facilitates anaerobic growth and biofilm formation in *N. gonorrhoeae.* Anaerobic respiration and biofilm formation facilitate persistent *N. gonorrhoeae* infections, reducing the efficacy of antibiotics. Thus, targeting AniA may enhance antibiotic efficacy. Understanding these mechanisms could also inform strategies to enhance antibiotic efficacy. Pajerski et al. [144] demonstrate that gold nanoparticles adhere to the bacterial cell wall and do not penetrate it in Gram-negative bacteria using scanning electron microscopy (SEM) and transmission electron microscopy (TEM). Thus, the interaction between GP-AuNPs and *N. gonorrhoeae* should be investigated to determine whether functionalization with a monoclonal antibody targeting a highly expressed surface protein on gonococci (e.g., porin B) should be considered to enhance specificity [145]. Badwaik et al. [146] further displayed how dextrose gold nanoparticles anchored to the outer surface of the bacterial cell wall and the sites where the gold nanoparticles had lodged showed the formation of perforations which resulted in complete cell lysis in *Escherichia-coli* (E-coli) (gram negative bacteria). Further highlighting the importance of investigating the interaction of GP-AuNPs with *N. gonorrhoeae.* Badwaik et al. [146] also demonstrated the damaging effects on the bacterial cell wall using propidium iodide to assess dye uptake in damaged cell walls resulting from membrane perturbation caused by the anchorage of gold nanoparticles. The largest dextrose gold nanoparticles (120 nm), which formed more perforations in the bacterial cell wall, displayed 92 % propidium iodide fluorescence, suggesting that larger gold nanoparticles have enhanced antibacterial activity. Thus, the effect of GP-AuNPs of varying sizes should be investigated to determine their effect on cell wall integrity and propidium iodide internalization. In terms of synthesis, the current study produced GP-AuNPs using a continuous stirring and heating method. Microfluidic synthesis could serve as an alternative, offering improved control over flow, temperature, particle size uniformity, polydispersity, and stability [147]. Although microfluidic green synthesis of gold nanoparticles has not yet been reported, it may provide advantages for scaled-up production. Additionally, while GP-AuNPs were stabilized with gum arabic, functionalization with chitosan could further enhance both specificity and stability [148]. Other avenues for optimization include the use of organic polymers, such as poly (lactic--co-glycolic acid) (PLGA) or PEG, as carriers or to form hybrid nanoparticles, which could potentially reduce cytotoxicity [92,149]. Future studies should also explore *in vivo* models. Li et al. [150] developed a human CEACAM1 transgenic mouse model (hu-CEACAM1) to study *N. gonorrhoeae* infection and drug mechanisms, which could be valuable for assessing GP-AuNP efficacy and safety. Moreover, while the HeLa cell line was used in this study, *N. gonorrhoeae* preferentially colonizes endocervical epithelial cells in females and urethral epithelial cells in males [109,142]. Thus, evaluating GP and GP-AuNPs on these cell types would be beneficial, as these cells express surface receptors and innate immune responses that occur during human infection.

4. Conclusion

This study is the first to use *G. perpensa* gold nanoparticles (GP-AuNPs) against *N. gonorrhoeae* and the first to assess the cytotoxicity of GP-AuNPs on selected cell lines, offering valuable insight into their therapeutic applicability. The study is of great significance in developing GP-AuNPs to target *N. gonorrhoeae,* a pathogen of growing global concern due to rising antibiotic resistance. Both GP and GP-AuNPs exhibited anti-gonococcal activity; however, the AuNPs had significant antibacterial activity against *N. gonorrhoeae*. This showed that the GP-AuNPs exhibited greater bioactivity than the crude extract. Furthermore, the GP-AuNPs were found to be selective towards *N. gonorrhoeae* compared to non-cancerous cell lines and less selective towards HeLa cells. Thus, the GP-AuNPs may be considered for the treatment of gonorrhoea but not STD-related cancers, such as cervical cancer. No published studies were found that investigated the anti-gonococcal activity of AuNPs synthesized using plants.

Despite these promising results, several limitations must be acknowledged. First, the current study was limited to *in vitro* assessments; thus, the observed antibacterial and cytotoxic effects may not fully translate to *in vivo* settings. The precise mechanisms by which GP-AuNPs exert their antibacterial effects remain unclear. Without data on reactive oxygen species (ROS) generation, membrane disruption, or interactions with bacterial proteins or DNA, mechanistic insights are limited.

In the future, organic polymers such as poly (lactic-co-glycolic acid) (PLGA) may be considered as carriers for GP to eliminate or reduce the cytotoxic effects of GP-AuNPs on non-cancerous cells in this study. Potentially improve synthesis using microfluidic synthesis to enhance AuNP quality and up-scale production. The GP-AuNPs themselves may also serve as promising candidates for the development of novel therapeutics against *N. gonorrhoeae*, particularly if supported by mechanistic studies elucidating their immunomodulatory properties. In this context, it would be valuable to investigate their potential to modulate host immune responses and reduce the chronic inflammatory state associated with gonococcal infection, a key factor contributing to disease persistence. Further studies evaluating the generation of reactive oxygen species (ROS) in *N. gonorrhoeae* in response to GP-AuNPs could help elucidate their antibacterial mechanisms of action. Additionally, examining the impact of GP-AuNPs on the expression of gonococcal

virulence factors such as Opa proteins, AniA, and the MtrCDE efflux pump, which drive adhesion, biofilm formation, and antibiotic resistance. Targeting AniA and MtrCDE could disrupt persistent infections and enhance antibiotic efficacy. To translate these findings into clinical application, *in vivo* studies assessing both the therapeutic efficacy and systemic toxicity of GP-AuNPs will be essential. Although GP alone exhibited comparatively weaker anti-gonococcal activity than its nanoparticle conjugate, it may still warrant further investigation as a potential therapeutic agent. In particular, future phytochemical analyses aimed at isolating and characterising individual bioactive compounds within GP could identify constituents with enhanced antimicrobial properties.

CRediT authorship contribution statement

Tanyaradzwa Tiandra Dembetembe: Writing – review & editing, Writing – original draft, Visualization, Methodology, Formal analysis, Conceptualization. **Danielle Twilley:** Writing – review & editing, Methodology. **Jacqueline Maphutha:** Methodology. **Marco Nuno De Canha:** Methodology. **Velaphi Clement Thipe:** Methodology. **Vusani Mandiwana:** Validation, Methodology. **Michel Lonji Kalombo:** Methodology. **Rirhandzu Rikhotso:** Visualization, Methodology. **Suprakas Sinha Ray:** Supervision. **Namrita Lall:** Supervision, Funding acquisition. **Quenton Kritzinger:** Supervision.

Funding

This research was supported by the National Research Foundation and the Department of Science and Innovation South African Research Chairs Initiative (NRF-SARChI: Grant No. SARCI150227114490).

Declaration of competing interest

The authors declare that they have no known competing financial interests or personal relationships that could have appeared to influence the work reported in this paper.

Acknowledgements

The authors would like to thank TDr Lulama Msinga who provided the indigenous knowledge which formed the basis of this study. We extend our gratitude to Ms Gill Whittington-Banda and the Edakeni Muthi Futhi Trust for supplying the plant material used in the study.

Data availability

The raw data supporting the conclusions of this article will be made available by the authors, without undue reservation to any qualified researcher.

References

[1] WHO Regional Office for Africa, Global health sector strategy on sexually transmitted infections 2016-2021 implementation framework for the African region, Brazzaville (2018). https://www.afro.who.int/publications/global-health-sector-strategy-sexually-transmitted-infections-2016-2021-implementation. (Accessed 2 April 2025).

[2] World Health Organization, Sex. Transm. Infect. (2024). https://www.who.int/news-room/fact-sheets/detail/sexually-transmitted-infections-(stis. (Accessed 15 January 2025).

[3] J. Rowley, S. Vander Hoorn, E. Korenromp, N. Low, M. Unemo, L.J. Abu-Raddad, R.M. Chico, A. Smolak, L. Newman, S. Gottlieb, S. Thwin, N. Broutet, M. M. Taylor, Global and regional estimates of the prevalence and incidence of four curable sexually transmitted infections in 2016, WHO Bull. 97 (2019) 548–562, https://doi.org/10.2471/BLT.18.228486.

[4] R. Kularatne, R. Niit, J. Rowley, T. Kufa-Chakezha, R.P. Peters, M.M. Taylor, L. F. Johnson, E.L. Korenromp, Adult gonorrhea, chlamydia and syphilis prevalence, incidence, treatment and syndromic case reporting in South Africa: estimates using the spectrum-STI model, 1990-2017, PLoS One 13 (2018) e0205863, https://doi.org/10.1371/journal.pone.0205863.

[5] R.D. Kirkcaldy, E. Weston, A.C. Segurado, G. Hughes, Epidemiology of gonorrhoea: a global perspective, Sex. Health 16 (2019) 401–411, https://doi.org/10.1071/SH19061.

[6] R. Kularatne, T. Kufa-Chakezha, V. Maseko, F. Gumede, *Neisseria gonorrhoeae* antimicrobial resistance surveillance: NICD GERMS-SA 2017, Commun. Dis. Surveillance Bull. 16 (2018) 131–139.

[7] I. Martin, P. Sawatzky, V. Allen, B. Lefebvre, L. Hoang, P. Naidu, J. Minion, P. van Caeseele, D. Haldane, R. Gad, G. Zahariadis, A. Corriveau, G. German, K. Tomas, M. Mulvey, Multidrug-resistant and extensively drug-resistant *Neisseria gonorrhoeae* in Canada, 2012–2016, Can. Commun. Dis. Rep. 45 (2019) 45–53, https://doi.org/10.14745/ccdr.v45i23a01.

[8] S.H. Yakobi, Y.B. Magibile, O.J. Pooe, A systematic review of *Neisseria gonorrhoeae* drug resistance development in South Africa, Braz. J. Microbiol. 55 (2024) 1053–1063, https://doi.org/10.1007/s42770-024-01281-6.

[9] B.S. Shim, Current concepts in bacterial sexually transmitted diseases, Kor. J. Urol. 52 (2011) 589–597, https://doi.org/10.4111/kju.2011.52.9.589.

[10] S.J. Quillin, H.S. Seifert, *Neisseria gonorrhoeae* host adaptation and pathogenesis, Nat. Rev. Microbiol. 16 (2018) 226–240, https://doi.org/10.1038/nrmicro.2017.169.

[11] Q. Yu, E.M. Chow, S.E. McCaw, N. Hu, D. Byrd, T. Amet, S. Hu, M.A. Ostrowski, S. Gray-Owen, Association of *Neisseria gonorrhoeae* OpaCEA with dendritic cells suppresses their ability to elicit an HIV-1-specific T cell memory response, PLoS One 8 (2013) e56705, https://doi.org/10.1371/journal.pone.0056705.

[12] M. Sadarangani, A.J. Pollard, S.D. Gray-Owen, Opa proteins and CEACAMs: pathways of immune engagement for pathogenic *Neisseria*, FEMS Microbiol. Rev. 35 (2011) 498–514, https://doi.org/10.1111/j.1574-6976.2010.00260.x.

[13] G.L. Murphy, T.D. Connell, D.S. Barritt, M. Koomey, J.G. Cannon, Phase variation of gonococcal protein II: regulation of gene expression by slipped-strand mispairing of a repetitive DNA sequence, Cell 56 (1989) 539–547, https://doi.org/10.1016/0092-8674(89)90577-1.

[14] E. Alirol, T.E. Wi, M. Bala, M.L. Bazzo, X. Chen, C. Deal, J.R. Dillon, R. Kularatne, J. Heim, R. Hooft Van Huijsduijnen, E. Hook, M.M. Lahra, D.A. Lewis, F. Ndowa, W. Shafer, L. Tayler, K. Workowski, M. Unemo, M. Balasegaram, Multidrug-resistant gonorrhea: a research and development roadmap to discover new medicines, PLoS Med. 14 (2017) e1002366, https://doi.org/10.1371/journal.pmed.1002366.

[15] P. Crowther-Gibson, N. Govender, D.A. Lewis, C. Bamford, A. Brink, A. von Gottberg, K. Klugman, M. du Plessis, A. Fali, B. Harris, K. Keddy, M. Botha, Part IV. GARP: human infections and antibiotic resistance, S. Afr. Med. J. 101 (2011) 567–578. http://www.samj.org.za/index.php/samj/article/view/5102/3367.

[16] V. Ouk, L.S. Heng, M. Virak, S. Deng, M.M. Lahra, R. Frankson, K. Kreisel, R. McDonald, M. Escher, M. Unemo, T. Wi, I. Maatouk, P. Penh, V. Fensham, E. Kersh, P. Cavailler, Y. Mundade, S.J. van Hal, R.L. Kundu, T.R. Hogan, D. M. Whiley, K. Izumi, T. Nishijima, High prevalence of ceftriaxone-resistant and XDR *Neisseria gonorrhoeae* in several cities of Cambodia, 2022–23: WHO Enhanced Gonococcal Antimicrobial Surveillance Programme (EGASP), JAC Antimicrob. Resist. 6 (2024), https://doi.org/10.1093/jacamr/dlae053.

[17] A. Palmeira-de-Oliveira, B.M. Silva, R. Palmeira-de-Oliveira, J. Martinez-de-Oliveira, L. Salgueiro, Are plant extracts a potential therapeutic approach for genital infections? Curr. Med. Chem. 20 (2013) 2914–2928, https://doi.org/10.2174/09298673113209990007.

[18] S. Yang, T. Wu, J. Zheng, Y. Huang, X.Y. Chen, H. Wu, Traditional Chinese medicinal herbs for *Condyloma acuminatum*, Cochrane Database Syst. Rev. (2012), https://doi.org/10.1002/14651858.CD010234.

[19] N.I. Mongalo, L.J. McGaw, J.F. Finnie, J. van Staden, Pharmacological properties of extracts from six South African medicinal plants used to treat sexually transmitted infections (STIs) and related infections, South Afr. J. Bot. 112 (2017) 290–295, https://doi.org/10.1016/j.sajb.2017.05.031.

[20] K.C. Chinsembu, Ethnobotanical study of medicinal flora utilised by traditional healers in the management of sexually transmitted infections in Sesheke district, Western province, Zambia, Rev. Bras Farmacogn. 26 (2016) 268–274, https://doi.org/10.1016/j.bjp.2015.07.030.

[21] H. de Wet, V.N. Nzama, S.F. van Vuuren, Medicinal plants used for the treatment of sexually transmitted infections by lay people in northern Maputaland, KwaZulu-Natal province, South Africa, South Afr. J. Bot. 78 (2012) 12–20, https://doi.org/10.1016/j.sajb.2011.04.002.

[22] P.O. Bessong, C.L. Obi, M.L. Andréola, L.B. Rojas, L. Pouységu, E. Igumbor, J.J. M. Meyer, S. Quideau, S. Litvak, Evaluation of selected South African medicinal plants for inhibitory properties against human immunodeficiency virus type 1 reverse transcriptase and integrase, J. Ethnopharmacol. 99 (2005) 83–91, https://doi.org/10.1016/j.jep.2005.01.056.

[23] B.E. van Wyk, B. van Oudtshoorn, N. Gericke, Medicinal Plants of South Africa, second ed., Briza, Pretoria, 2017.

[24] L. Kambizi, N. Sultana, A.J. Afolayan, Bioactive compounds isolated from *Aloe ferox*: a plant traditionally used for the treatment of sexually transmitted infections in the Eastern Cape, South Africa, Pharm. Biol. 42 (2005) 636–639, https://doi.org/10.1080/13880200490902581.

[25] S. Semenya, M.J. Potgieter, L.J.C. Erasmus, Bapedi phytomedicine and their use in the treatment of sexually transmitted infections in Limpopo province, South Africa, Afr J. Pharm. Pharmacol. 7 (2013) 250–262, https://doi.org/10.5897/AJPP12.608.

[26] A.N. Yilma, S.R. Singh, S. Dixit, V.A. Dennis, Anti-inflammatory effects of silver-polyvinyl pyrrolidone (Ag-PVP) nanoparticles in mouse macrophages infected with live *Chlamydia trachomatis*, Int. J. Nanomed. 8 (2013) 2421–2432.

[27] L.H. Li, M.Y. Yen, C.C. Ho, P. Wu, C.C. Wang, P.K. Maurya, P.S. Chen, W. Chen, W.Y. Hsieh, H.W. Chen, Non-cytotoxic nanomaterials enhance antimicrobial

activities of cefmetazole against multidrug-resistant *Neisseria gonorrhoeae*, PLoS One 8 (2013) e64794, https://doi.org/10.1371/journal.pone.0064794.
[28] S. Rossi, B. Vigani, G. Sandri, M.C. Bonferoni, C.M. Caramella, F. Ferrari, Recent advances in the mucus-interacting approach for vaginal drug delivery: from mucoadhesive to mucus-penetrating nanoparticles, Expet Opin. Drug Deliv. 16 (2019) 777–781, https://doi.org/10.1080/17425247.2019.1645117.
[29] R.A. Cone, Barrier properties of mucus, Adv. Drug Deliv. Rev. 61 (2009) 75–85, https://doi.org/10.1016/j.addr.2008.09.008.
[30] S. Krishna, V. Ashok, A. Chatterjee, A review on vaginal drug delivery systems, Int. J. Biol. Pharm. Allied Sci. 1 (2012) 152–167.
[31] M.I. Lucío, M.-E. Kyriazi, J. Hamilton, D. Batista, A. Sheppard, E. Sams-Dodd, M. V. Humbert, I. Hussain, M. Christodoulides, A.G. Kanaras, Bactericidal effect of 5-mercapto-2-nitrobenzoic acid-coated silver nanoclusters against multidrug-resistant *Neisseria gonorrhoeae*, ACS Appl. Mater. Interfaces 12 (2020) 27994–28003, https://doi.org/10.1021/acsami.0c06163.
[32] T.-Y. Yang, S.-P. Tseng, H.-C. Ho, L.-H. Chen, P.-R. Hsueh, P.-L. Lu, C.-H. Lin, L.-C. Wang, *In vitro* evaluation of tellurium-based AS101 compound against *Neisseria gonorrhoeae* infectivity, Microbiol. Spectr. 11 (2023) e0149622, https://doi.org/10.1128/spectrum.01496-22.
[33] F. Alqahtani, F. Aleanizy, E. El Tahir, H. Alhabib, R. Alsaif, G. Shazly, H. AlQahtani, I. Alsarra, J. Mahdavi, Antibacterial activity of chitosan nanoparticles against pathogenic *N. gonorrhoea*, Int. J. Nanomed. 15 (2020) 7877–7887, https://doi.org/10.2147/IJN.S272736.
[34] L.-H. Li, M.-Y. Yen, C.-C. Ho, P. Wu, C.-C. Wang, P.K. Maurya, P.-S. Chen, W. Chen, W.-Y. Hsieh, H.-W. Chen, Non-cytotoxic nanomaterials enhance antimicrobial activities of cefmetazole against multidrug-resistant *Neisseria gonorrhoeae*, PLoS One 8 (2013) e64794, https://doi.org/10.1371/journal.pone.0064794.
[35] L.M. Ensign, R. Cone, J. Hanes, Nanoparticle-based drug delivery to the vagina: a review, J. Contr. Release 190 (2014) 500–514, https://doi.org/10.1016/j.jconrel.2014.04.033.
[36] H.H. Lara, N.V. Ayala-Nuñez, L. Ixtepan-Turrent, C. Rodriguez-Padilla, Mode of antiviral action of silver nanoparticles against HIV-1, J. Nanobiotechnol. 8 (2010) 1, https://doi.org/10.1186/1477-3155-8-1.
[37] R. Kesarkar, L-Cysteine functionalized gold nanocargos potentiates anti-HIV activity of azidothymydine against HIV-1Ba-L virus, J. Immuno. Virol. 1 (2015) 555552, https://doi.org/10.19080/jojiv.2015.01.555552.
[38] R. Gholizadeh, S. Mosleh-Shirazi, A.M. Amani, Investigation of electrospun chitosan nanofibers reinforced with mesoporous silicon oxide decorated with silver nanoparticles in diabetic wound treatment, Int. J. Biol. Macromol. 322 (2025) 146432, https://doi.org/10.1016/j.ijbiomac.2025.146432.
[39] S. Montazersaheb, A. Eftekhari, A. Shafaroodi, S. Tavakoli, S. Jafari, A. Baran, M. F. Baran, S. Jafari, E. Ahmadian, Green-synthesized silver nanoparticles from peel extract of pumpkin as a potent radiosensitizer against triple-negative breast cancer (TNBC), Cancer Nanotechnol. 15 (2024) 47, https://doi.org/10.1186/s12645-024-00285-z.
[40] V.C. Thipe, K.P. Amiri, P. Bloebaum, A.R. Karikachery, M. Khoobchandani, K. K. Katti, S.S. Jurisson, K.V. Katti, Development of resveratrol-conjugated gold nanoparticles: interrelationship of increased resveratrol corona on anti-tumor efficacy against breast, pancreatic and prostate cancers, Int. J. Nanomed. 14 (2019) 4413–4428, https://doi.org/10.2147/IJN.S204443.
[41] R. Javed, M. Zia, S. Naz, S.O. Aisida, N. ul Ain, Q. Ao, Role of capping agents in the application of nanoparticles in biomedicine and environmental remediation: recent trends and future prospects, J. Nanobiotechnol. 18 (2020) 172, https://doi.org/10.1186/s12951-020-00704-4.
[42] D.B. Chithrani, W.C. Chan, Elucidating the mechanism of cellular uptake and removal of protein-coated gold nanoparticles of different sizes and shapes, Nano Lett. 7 (2007) 1542–1550, https://doi.org/10.1021/nl070363y.
[43] S. Ying, Z. Guan, P.C. Ofoegbu, P. Clubb, C. Rico, F. He, J. Hong, Green synthesis of nanoparticles: current developments and limitations, Environ. Technol. Innov. 26 (2022) 102336, https://doi.org/10.1016/j.eti.2022.102336.
[44] S. Khare, R.K. Singh, O. Prakash, Green synthesis, characterization and biocompatibility evaluation of silver nanoparticles using radish seeds, Results Chem. 4 (2022) 100447, https://doi.org/10.1016/j.rechem.2022.100447.
[45] D. Baram-Pinto, S. Shukla, A. Gedanken, R. Sarid, Inhibition of HSV-1 attachment, entry, and cell-to-cell spread by functionalized multivalent gold nanoparticles, Small 6 (2010) 1044–1050, https://doi.org/10.1002/smll.200902384.
[46] P. Di Gianvincenzo, M. Marradi, O.M. Martínez-Ávila, L.M. Bedoya, J. Alcamí, S. Penadés, Gold nanoparticles capped with sulfate-ended ligands as anti-HIV agents, Bioorg. Med. Chem. Lett 20 (2010) 2718–2721, https://doi.org/10.1016/j.bmcl.2010.03.079.
[47] J.K. Patra, Y. Kwon, K.-H. Baek, Green biosynthesis of gold nanoparticles by onion peel extract: synthesis, characterization and biological activities, Adv. Powder Technol. 27 (2016) 2204–2213, https://doi.org/10.1016/j.apt.2016.08.005.
[48] N. Patel, K. Kasumbwe, V. Mohanlall, S.L. Mbatha, Antibacterial of *Gunnera perpensa*-mediated silver nanoparticles, J. Nanotechnol. 2020 (2020) 4508543, https://doi.org/10.1155/2020/4508543.
[49] A. Dhanasezhian, S. Srivani, K. Govindaraju, P. Preetam, S. Sasikala, M. R. Rameshkumar, Anti-herpes simplex virus (HSV-1 and HSV-2) activity of biogenic gold and silver nanoparticles using seaweed *Sargassum wightii*, Indian J. Geomarine Sci. 48 (2019) 1252–1257.
[50] B.A. Aderibigbe, Metal-based nanoparticles for the treatment of infectious diseases, Molecules 22 (2017) 1370, https://doi.org/10.3390/molecules22081370.
[51] M. Saed, R.D. Ayivi, J. Wei, S.O. Obare, Gold nanoparticles antibacterial activity: does the surface matter? Colloid Interface Sci. Commun. 62 (2024) 100804 https://doi.org/10.1016/j.colcom.2024.100804.
[52] F.K. Mammo, V. Mohanlall, F.O. Shode, perpensa L. Gunnera, A multi-use ethnomedicinal plant species in South Africa, Afr J. Sci. Technol. Innov. Dev. 9 (2017) 77–83, https://doi.org/10.1080/20421338.2016.1269458.
[53] T.H. Arnold, B.C. de Wet, Plants of Southern Africa: Names and Distribution, first ed., National Botanical Institute, Pretoria, 1993.
[54] W.B. Silvester, D.R. Smith, Nitrogen fixation by *Gunnera*–nostoc symbiosis, Nature 224 (1969) 1231, https://doi.org/10.1038/2241231a0.
[55] K.B. Brookes, M.F. Dutton, Bioactive components of the uteroactive medicinal plant, *Gunnera perpensa* (or ugobo), South Afr. J. Sci. 103 (2007) 187–189. http://www.scielo.org.za/scielo.php?script=sci_arttext&pid=S0038-23532007000300007. (Accessed 18 August 2019).
[56] L.V. Buwa, J. van Staden, Antibacterial and antifungal activity of traditional medicinal plants used against venereal diseases in South Africa, J. Ethnopharmacol. 103 (2006) 139–142, https://doi.org/10.1016/j.jep.2005.09.020.
[57] A. Maroyi, From traditional usage to pharmacological evidence: systematic review of *Gunnera perpensa*L, Evid. base Compl. Alternative Med. 2016 (2016) 1–14, https://doi.org/10.1155/2016/1720123.
[58] T. Dembetembe, S. Rademan, D. Twilley, G.W. Banda, L. Masinga, N. Lall, Q. Kritzinger, Antimicrobial and cytotoxic effects of medicinal plants traditionally used for the treatment of sexually transmitted diseases, South Afr. J. Bot. 154 (2023), https://doi.org/10.1016/j.sajb.2023.01.042.
[59] M. Hu, J. Chen, Z.-Y. Li, L. Au, G.V. Hartland, X. Li, M. Marquez, Y. Xia, Gold nanostructures: engineering their plasmonic properties for biomedical applications, Chem. Soc. Rev. 35 (2006) 1084, https://doi.org/10.1039/b517615h.
[60] M.N. De Canha, V.C. Thipe, K. V Katti, V. Mandiwana, M.L. Kalombo, S.S. Ray, R. Rikhotso, A.J. Van Vuuren, N. Lall, The activity of gold nanoparticles synthesized using *Helichrysum odoratissimum* against *Cutibacterium acnes* biofilms, Front. Cell Dev. Biol. 9 (2021) 675064, https://doi.org/10.3389/fcell.2021.675064.
[61] P. Cos, J. Vlietinck, Arnold, D. Varden Berghe, L. Maes, Anti-infective potential of natural products: how to develop a stronger *in vitro* "proof-of-concept, J. Ethnopharmacol. 106 (2006) 290–302, https://doi.org/10.1016/j.jep.2006.04.003.
[62] T.E. Tshikalange, P. Mamba, S.A. Adebayo, Antimicrobial, antioxidant and cytotoxicity studies of medicinal plants used in the treatment of sexually transmitted diseases, Int. J. Pharmacogn. Phytochem. Res. 8 (2016) 1891–1895.
[63] J.N. Eloff, A sensitive and quick microplate method to determine the minimal inhibitory concentration of plant extracts for bacteria, Planta Med. 64 (1998) 711–713, https://doi.org/10.1055/s-2006-957563.
[64] N. Lall, C.J. Henley-Smith, M.N. De Canha, C.B. Oosthuizen, D. Berrington, Viability reagent prestoblue compared with other available reagents used in cytotoxicity and antimicrobial assays, Internet J. Microbiol. 148 (2013) 45–55, https://doi.org/10.1155/2013/420601.
[65] A.J. Shnoudeh, I. Hamad, R.W. Abdo, L. Qadumii, A.Y. Jaber, H.S. Surchi, S. Z. Alkelany, Synthesis, characterization, and applications of metal nanoparticles, in: Rakesh K. Tekade (Ed.), Biomaterials and Bionanotechnology, first ed., Elsevier, London, 2019, pp. 527–612, https://doi.org/10.1016/B978-0-12-814427-5.00015-9.
[66] A. Blom van Staden, D. Kovacs, G. Cardinali, M. Picardo, M. Lebeko, N. C. Khumalo, S.S. Ray, N. Lall, Synthesis and characterization of gold nanoparticles biosynthesised from *Aspalathus linearis* (Burm.f.) R.Dahlgren for progressive macular hypomelanosis, J. Herb. Med. 29 (2021) 100481, https://doi.org/10.1016/j.hermed.2021.100481.
[67] B.S. Srinath, V. Ravishankar Rai, Biosynthesis of highly monodispersed, spherical gold nanoparticles of size 4–10 nm from spent cultures of *Klebsiella pneumoniae*, 3 Biotech 5 (2015) 671–676, https://doi.org/10.1007/s13205-014-0265-2.
[68] A.A. Ashkarran, A. Bayat, Surface plasmon resonance of metal nanostructures as a complementary technique for microscopic size measurement, Int. Nano Lett. 3 (2013) 1–10, https://doi.org/10.1186/2228-5326-3-50.
[69] P. Bélteky, A. Rónavári, D. Zakupszky, E. Boka, N. Igaz, B. Szerencsés, I. Pfeiffer, C. Vágvölgyi, M. Kiricsi, Z. Kónya, Are smaller nanoparticles always better? Understanding the biological effect of size-dependent silver nanoparticle aggregation under biorelevant conditions, Int. J. Nanomed. 16 (2021) 3021–3040, https://doi.org/10.2147/IJN.S304138.
[70] M.A. Dheyab, A.A. Aziz, P.M. Khaniabadi, M.S. Jameel, N. Oladzadabbasabadi, S. A. Mohammed, R.S. Abdullah, B. Mehrdel, Monodisperse gold nanoparticles: a review on synthesis and their application in modern medicine, Int. J. Mol. Sci. 23 (2022) 7400, https://doi.org/10.3390/IJMS23137400.
[71] H. Kaur, H. Kaur, A. Sharma, Study of SPR peak shifting of silver nanoparticles with change in surrounding medium, Mater. Today Proc. 37 (2021) 3574–3576, https://doi.org/10.1016/J.MATPR.2020.09.584.
[72] R. Thilagam, A. Gnanamani, Preparation, characterization and stability assessment of keratin and albumin functionalized gold nanoparticles for biomedical applications, Appl. Nanosci. 10 (2020) 1879–1892, https://doi.org/10.1007/S13204-020-01250-Z.
[73] S.M. Bloom, N.A. Mafunda, B.M. Woolston, M.R. Hayward, J.F. Frempong, A. B. Abai, J. Xu, A.J. Mitchell, X. Westergaard, F.A. Hussain, N. Xulu, M. Dong, K. L. Dong, T. Gumbi, F.X. Ceasar, J.K. Rice, N. Choksi, N. Ismail, T. Ndung'u, M. S. Ghebremichael, D.A. Relman, E.P. Balskus, C.M. Mitchell, D.S. Kwon, Cysteine dependence of *Lactobacillus iners* is a potential therapeutic target for vaginal

microbiota modulation, Nat. Microbiol. 7 (2022) 434–450, https://doi.org/10.1038/s41564-022-01070-7.
[74] R.N. Wadetwar, P.S. Kanojiya, Vaginal nano-based drug delivery system, in: Vivek Dave, Nikita Gupta, Srija Sur (Eds.), Nanopharmaceutical Advanced Delivery Systems, first ed., Wiley-Scrivener, Beverly, 2021, pp. 357–377, https://doi.org/10.1002/9781119711698.ch16.
[75] M. Herzberg, C.A. Jöel, A. Katchalsky, The cyclic variation of sodium chloride content in the mucus of the cervix uteri, Fertil. Steril. 15 (1964) 684–694, https://doi.org/10.1016/S0015-0282(16)35414-0.
[76] G. Lacroix, V. Gouyer, F. Gottrand, J.-L. Desseyn, The cervicovaginal mucus barrier, Int. J. Mol. Sci. 21 (2020) 8266, https://doi.org/10.3390/ijms21218266.
[77] M. Fuller, I. Köper, Polyelectrolyte-coated gold nanoparticles: the effect of salt and polyelectrolyte concentration on colloidal stability, Polymers 10 (2018) 1336, https://doi.org/10.3390/polym10121336.
[78] A.M. Smith, A.A. Lee, S. Perkin, The electrostatic screening length in concentrated electrolytes increases with concentration, J. Phys. Chem. Lett. (2016) 2157–2163, https://doi.org/10.1021/ACS.JPCLETT.6B00867.
[79] D.A. Bryant, Debye length in a kappa-distribution plasma, J. Plasma Phys. 56 (1996) 87–93, https://doi.org/10.1017/S0022377800019115.
[80] E.V. Stenson, J. Horn-Stanja, M.R. Stoneking, T.S. Pedersen, Debye length and plasma skin depth: two length scales of interest in the creation and diagnosis of laboratory pair plasmas, J. Plasma Phys. 83 (2017), https://doi.org/10.1017/S0022377817000022.
[81] D.N. Williams, K.A. Gold, T.R.P. Holoman, S.H. Ehrman, O.C. Wilson, Surface modification of magnetic nanoparticles using gum arabic, J. Nano Res. 8 (2006) 749–753, https://doi.org/10.1007/s11051-006-9084-7.
[82] H.H. Musa, A.A. Ahmed, T.H. Musa, Chemistry, biological, and pharmacological properties of gum arabic, in: J.-M. Mérillon, K.G. Ramawat (Eds.), Bioactive Molecules in Food, Springer, Cham, 2019, pp. 797–814, https://doi.org/10.1007/978-3-319-78030-6_11. (Accessed 1 March 2021).
[83] R.C. Randall, G.O. Phillips, P.A. Williams, The role of the proteinaceous component on the emulsifying properties of gum arabic, Food Hydrocoll. 2 (1988) 131–140, https://doi.org/10.1016/S0268-005X(88)80011-0.
[84] M. Danaei, M. Dehghankhold, S. Ataei, F. Hasanzadeh Davarani, R. Javanmard, A. Dokhani, S. Khorasani, M.R. Mozafari, Impact of particle size and polydispersity index on the clinical applications of lipidic nanocarrier systems, Pharmaceutics 10 (2018) 57, https://doi.org/10.3390/pharmaceutics10020057.
[85] T. Mudalige, H. Qu, D. van Haute, S.M. Ansar, A. Paredes, T. Ingle, Characterization of nanomaterials: tools and challenges, in: A.L. Rubio, M. martínez Sanz, M.J.F. Rovira, L.G. Gómez-Mascaraque (Eds.), Nanomaterials for Food Applications, Elsevier, 2019, pp. 313–353.
[86] A.A. Ahmed, Health benefits of gum arabic and medical use, in: A.A. Mariod (Ed.), Gum Arabic: Structure, Properties, Application and Economics, Elsevier, London, 2018, pp. 183–210, https://doi.org/10.1016/B978-0-12-812002-6.00016-6.
[87] A.M. Gamal-Eldeen, D. Moustafa, S.M. El-Daly, E.A. El-Hussieny, S. Saleh, M. Khoobchandani, K.L. Bacon, S. Gupta, K. Katti, R. Shukla, K.V. Katti, Photothermal therapy mediated by gum arabic-conjugated gold nanoparticles suppresses liver preneoplastic lesions in mice, J. Photochem. Photobiol., B 163 (2016) 47–56, https://doi.org/10.1016/j.jphotobiol.2016.08.009.
[88] G. Leyva-Gómez, E. Piñón-Segundo, N. Mendoza-Muñoz, M.L. Zambrano-Zaragoza, S. Mendoza-Elvira, D. Quintanar-Guerrero, Approaches in polymeric nanoparticles for vaginal drug delivery: a review of the state of the art, Int. J. Mol. Sci. 19 (2018) e1549, https://doi.org/10.3390/ijms19061549.
[89] A.N. Geraldes, A.A. da Silva, J. Leal, G.M. Estrada-Villegas, N. Lincopan, K. V. Katti, A.B. Lug&atildeo, Green nanotechnology from plant extracts: synthesis and characterization of gold nanoparticles, Adv. Nanoparticles 5 (2016) 176–185, https://doi.org/10.4236/anp.2016.53019.
[90] J. Coates, Interpretation of infrared spectra, a practical approach, in: R.A. Meyers (Ed.), Encyclopedia of Analytical Chemistry, John Wiley & Sons, Chichester, 2000, pp. 10815–10837.
[91] A.B.D. Nandiyanto, R. Oktiani, R. Ragadhita, How to read and interpret FTIR spectroscope of organic material, Indonesian J. Sci. Technol. 4 (2019) 97–118, https://doi.org/10.17509/ijost.v4i1.15806.
[92] M. Yüce, H. Kurt, How to make nanobiosensors: surface modification and characterisation of nanomaterials for biosensing applications, RSC Adv. 7 (2017) 49386–49403, https://doi.org/10.1039/C7RA10479K.
[93] N. Hock, G.F. Racaniello, S. Aspinall, N. Denora, V. V Khutoryanskiy, A. Bernkop-Schnürch, N. Hock, G.F. Racaniello, N. Denora, A. Moro, Bari, I.S. Aspinall, V. V Khutoryanskiy, A. Bernkop-Schnürch, Thiolated nanoparticles for biomedical applications: mimicking the workhorses of our body, Adv. Sci. 9 (2022) 2102451, https://doi.org/10.1002/ADVS.202102451.
[94] L. Invernizzi, P. Moyo, J. Cassel, F.J. Isaacs, J.M. Salvino, L.J. Montaner, I. Tietjen, V. Maharaj, Use of hyphenated analytical techniques to identify the bioactive constituents of *Gunnera perpensa* L., a South African medicinal plant, which potently inhibit SARS-CoV-2 spike glycoprotein–host ACE2 binding, Anal. Bioanal. Chem. 414 (2022) 3971–3985, https://doi.org/10.1007/s00216-022-04041-3.
[95] F. Khan, X.K. Peter, R.M. Mackenzie, L. Katsoulis, R. Gehring, O.Q. Munro, F. R. van Heerden, S.E. Drewes, Venusol from *Gunnera perpensa*: structural and activity studies, Phytochemistry 65 (2004) 1117–1121, https://doi.org/10.1016/j.phytochem.2004.02.024.
[96] N. Mohamad Zain, I. Mohd Amin, F. Abdul Razak, M.I. Abu Hassan, Preliminary screening of pomegranate-derived compounds for antimicrobial and anti-virulence effects against cariogenic streptococci, Saudi Dent J. 37 (2025) 84, https://doi.org/10.1007/s44445-025-00083-2.
[97] B.C. Chigor, Development of Conservation Methods for *Gunnera perpensa* L.: an Overexploited Medicinal Plant in the Eastern Cape, University of Fort Hare, South Africa, 2014. https://www.semanticscholar.org/paper/Development-of-conservation-methods-for-Gunnera-L.%3A-Chigor/91342604bd1d58fe9e804617339c111aa78709f6. (Accessed 18 August 2019).
[98] A.B.D. Nandiyanto, R. Oktiani, R. Ragadhita, A. Sukmafitri, R. Zaen, Amorphous content on the photocatalytic performance of micrometer-sized tungsten trioxide particles, Arab. J. Chem. 13 (2020) 2912–2924, https://doi.org/10.1016/j.arabjc.2018.07.021.
[99] S.E. Drewes, F. Khan, S.F. van Vuuren, A.M. Viljoen, Simple 1,4-benzoquinones with antibacterial activity from stems and leaves of *Gunnera perpensa*, Phytochemistry 66 (2005) 1812–1816, https://doi.org/10.1016/j.phytochem.2005.05.024.
[100] H.K. Patra, S. Banerjee, U. Chaudhuri, P. Lahiri, A.K. Dasgupta, Cell selective response to gold nanoparticles, Nanomedicine 3 (2007) 111–119, https://doi.org/10.1016/j.nano.2007.03.005.
[101] A. Lobiuc, N.-E. Pavăl, I.I. Mangalagiu, R. Gheorghiță, G.-C. Teliban, D. Amăriucăi-Mantu, V. Stoleru, Future antimicrobials: natural and functionalized phenolics, Molecules 28 (2023) 1114, https://doi.org/10.3390/molecules28031114.
[102] U. Mabona, A. Viljoen, E. Shikanga, A. Marston, S. van Vuuren, Antimicrobial activity of southern African medicinal plants with dermatological relevance: from an ethnopharmacological screening approach, to combination studies and the isolation of a bioactive compound, J. Ethnopharmacol. 148 (2013) 45–55, https://doi.org/10.1016/j.jep.2013.03.056.
[103] N. Lall, K.M. Szuman, B. Madikizela, A.-M. Kok, M.N. De Canha, Extracts of southern African aquatic and wetland plant species as effective tyrosinase inhibitors, South Afr. J. Bot. 175 (2024) 574–586, https://doi.org/10.1016/j.sajb.2024.10.041.
[104] M.A.M. Hussein, M. Grinholc, A.S.A. Dena, I.M. El-Sherbiny, M. Megahed, Boosting the antibacterial activity of chitosan–gold nanoparticles against antibiotic–resistant bacteria by *Punicagranatum* L. extract, Carbohydr. Polym. 256 (2021) 1–11, https://doi.org/10.1016/j.carbpol.2020.117498.
[105] M.J. Hajipour, K.M. Fromm, A.A. Ashkarran, D. Jimenez De Aberasturi, I. Ruiz De Larramendi, T. Rojo, V. Serpooshan, W.J. Parak, M. Mahmoudi, Antibacterial properties of nanoparticles, Trends Biotechnol. 30 (2012) 499–511, https://doi.org/10.1016/j.tibtech.2012.06.004.
[106] A. Timoszyk, R. Grochowalska, Mechanism and antibacterial activity of gold nanoparticles (AuNPs) functionalized with natural compounds from plants, Pharmaceutics 14 (2022) 2599, https://doi.org/10.3390/pharmaceutics14122599.
[107] C. Keskin, S. Aslan, M.F. Baran, A. Baran, A. Eftekhari, M.T. Adıcan, E. Ahmadian, S. Arslan, A.J. Mohamed, Green synthesis and characterization of silver nanoparticles using *Anchusa officinalis*: antimicrobial and cytotoxic potential, Int. J. Nanomed. 20 (2025) 4481–4502, https://doi.org/10.2147/IJN.S511217.
[108] V. Kuete, T. Efferth, African flora has the potential to fight multidrug resistance of cancer, BioMed Res. Int. 2015 (2015) 914813, https://doi.org/10.1155/2015/914813.
[109] A. Elkashif, M.N. Seleem, Investigation of auranofin and gold-containing analogues antibacterial activity against multidrug-resistant *Neisseria gonorrhoeae*, Sci. Rep. 10 (2020) 1–9, https://doi.org/10.1038/s41598-020-62696-3.
[110] R. Lagha, F. Ben Abdallah, A. Mezni, O.M. Alzahrani, Effect of plasmonic gold nanoprisms on biofilm formation and heat shock proteins expression in human pathogenic bacteria, Pharmaceuticals 14 (2021) 1335, https://doi.org/10.3390/ph14121335.
[111] P. Mamba, S.A. Adebayo, T.E. Tshikalange, Anti-microbial, anti-inflammatory and HIV-1 reverse transcriptase activity of selected South African plants used to treat sexually transmitted diseases, Int. J. Pharmacogn. Phytochem. Res. 8 (2016) 1870–1876.
[112] J.H. Melendez, J. Hardick, M. Barnes, K.R. Page, C.A. Gaydos, Antimicrobial susceptibility of *Neisseria gonorrhoeae* isolates in Baltimore, Maryland, 2016: the importance of sentinel surveillance in the era of multi-drug-resistant gonorrhea, Antibiotics 7 (2018) 77, https://doi.org/10.3390/antibiotics7030077.
[113] S.F.E. Bell, R.S. Ware, D.A. Lewis, M.M. Lahra, D.M. Whiley, Antimicrobial susceptibility assays for *Neisseria gonorrhoeae*: a proof-of-principle population-based retrospective analysis, Lancet Microbe 4 (2023) 544–551, https://doi.org/10.1016/S2666-5247(23)00071-X.
[114] X. Li, S.M. Robinson, A. Gupta, K. Saha, Z. Jiang, D.F. Moyano, A. Sahar, M. A. Riley, V.M. Rotello, Functional gold nanoparticles as potent antimicrobial agents against multi-drug-resistant bacteria, ACS Nano 8 (2014) 10682–10686, https://doi.org/10.1021/nn5042625.
[115] A. Gürbay, C. Garrel, M. Osman, M.-J. Richard, A. Favier, F. Hincal, Cytotoxicity in ciprofloxacin-treated human fibroblast cells and protection by vitamin E, Hum. Exp. Toxicol. 21 (2002) 635–641, https://doi.org/10.1191/0960327102ht305oa.
[116] S.M.D. Rizvi, A.S.A. Lila, A. Moin, T. Hussain, M.A. Kamal, H. Sonbol, E.-S. Khafagy, Antibiotic-loaded gold nanoparticles: a nano-arsenal against ESBL producer-resistant pathogens, Pharmaceutics 15 (2023) 430, https://doi.org/10.3390/pharmaceutics15020430.
[117] A.I. Ribeiro, A.M. Dias, A. Zille, Synergistic effects between metal nanoparticles and commercial antimicrobial agents: a review, ACS Appl. Nano Mater. 5 (2022) 3030–3064, https://doi.org/10.1021/acsanm.1c03891.
[118] T.-F.C. Mah, G.A. O'Toole, Mechanisms of biofilm resistance to antimicrobial agents, Trends Microbiol. 9 (2001) 34–39, https://doi.org/10.1016/S0966-842X(00)01913-2.
[119] M. Christodoulides, J.S. Everson, B.L. Liu, P.R. Lambden, P.J. Watt, E.J. Thomas, J.E. Heckels, Interaction of primary human endometrial cells with *Neisseria*

gonorrhoeae expressing green fluorescent protein, Mol. Microbiol. 35 (2000) 32–43, https://doi.org/10.1046/j.1365-2958.2000.01694.x.
[120] A. Folorunso, S. Akintelu, A.K. Oyebamiji, S. Ajayi, B. Abiola, I. Abdusalam, A. Morakinyo, Biosynthesis, characterization and antimicrobial activity of gold nanoparticles from leaf extracts of *Annona muricata*, J. Nanostruct. Chem. 9 (2019) 111–117, https://doi.org/10.1007/s40097-019-0301-1.
[121] C. Garrido, C.A. Simpson, N.P. Dahl, J. Bresee, D.C. Whitehead, E.A. Lindsey, T. L. Harris, C.A. Smith, C.J. Carter, D.L. Feldheim, C. Melander, D.M. Margolis, Gold nanoparticles to improve HIV drug delivery, Future Med. Chem. 7 (2015) 1097–1107, https://doi.org/10.4155/FMC.15.57.
[122] F. Chiodo, M. Marradi, J. Calvo, E. Yuste, S. Penadés, Glycosystems in nanotechnology: gold glyconanoparticles as carrier for anti-HIV prodrugs, Beilstein J. Org. Chem. 10 (2014) 1339–1346, https://doi.org/10.3762/bjoc.10.136.
[123] M.-C. Bowman, T.E. Ballard, C.J. Ackerson, D.L. Feldheim, D.M. Margolis, C. Melander, Inhibition of HIV fusion with multivalent gold nanoparticles, J. Am. Chem. Soc. 130 (2008) 6896–6897, https://doi.org/10.1021/ja710321g.
[124] P. Boomi, R. Ganesan, G. Prabu Poorani, S. Jegatheeswaran, C. Balakumar, H. Gurumallesh Prabu, K. Anand, N. Marimuthu Prabhu, J. Jeyakanthan, M. Saravanan, Phyto-engineered gold nanoparticles (AuNPs) with potential antibacterial, antioxidant, and wound healing activities under *in vitro* and *in vivo* conditions, Int. J. Nanomed. 15 (2020) 7553–7568, https://doi.org/10.2147/IJN.S257499.
[125] M.R. Bindhu, M. Umadevi, Antibacterial activities of green synthesized gold nanoparticles, Mater. Lett. 120 (2014) 122–125, https://doi.org/10.1016/J.MATLET.2014.01.108.
[126] A. Al Saqr, E.S. Khafagy, A. Alalaiwe, M.F. Aldawsari, S.M. Alshahrani, M. K. Anwer, S. Khan, A.S. Abu Lila, H.H. Arab, W.A.H. Hegazy, Synthesis of gold nanoparticles by using green machinery: characterization and *in vitro* toxicity, Nanomaterials 11 (2021) 1–14, https://doi.org/10.3390/NANO11030808.
[127] B. Diedericks, A.-M. Kok, V. Mandiwana, B.G. Gordhan, B.D. Kana, S.S. Ray, N. Lall, Antitubercular activity of 7-methyljuglone-loaded poly-(lactide co-glycolide) nanoparticles, Pharmaceutics 16 (2024) 1477, https://doi.org/10.3390/pharmaceutics16111477.
[128] C.-Y. Xiao, B.-B. Fu, Z.-Y. Li, G. Mushtaq, M.A. Kamal, J.-H. Li, G.-C. Tang, S.-S. Xiao, Observations on the expression of human papillomavirus major capsid protein in HeLa cells, Cancer Cell Int. 15 (2015) 53, https://doi.org/10.1186/s12935-015-0206-0.
[129] Z. Sun, Y. Sun, Y. Li, X. Luan, H. Chen, H. Wu, B. Peng, C. Lu, Identification of HeLa cell proteins that interact with *Chlamydia trachomatis* glycogen synthase using yeast two-hybrid assays, Mol. Med. Rep. 21 (2020) 1572–1580, https://doi.org/10.3892/mmr.2020.10947.
[130] M. Heydarian, E. Rühl, R. Rawal, V. Kozjak-Pavlovic, Tissue models for *Neisseria gonorrhoeae* research—from 2D to 3D, Front. Cell. Infect. Microbiol. 12 (2022) 840122, https://doi.org/10.3389/fcimb.2022.840122.
[131] M. Mwale, P.J. Masika, Toxicity evaluation of the aqueous leaf extract of *Gunnera perpensa* L. (Gunneraceae), Afr. J. Biotechnol. 10 (2011) 2503–2513, https://doi.org/10.2503-2513.
[132] P.-M.-A. Mfengwana, S.S. Mashele, I. Manduna, In vitro antibacterial, antioxidant and anti-inflammatory effects of *Senecio asperulus* and *Gunnera perpensa* from Mohale's Hoek, Lesotho, Pharmacogn. J. 11 (2019) 730–739, https://doi.org/10.5530/pj.2019.11.116.
[133] M. Simelane, O. Lawal, T. Djarova, C. Musabayane, M. Singh, A. Opoku, Lactogenic activity of rats stimulated by *Gunnera perpensa* L. (Gunneraceae) from South Africa, Afr. J. Tradit., Complementary Altern. Med. 9 (2012) 561–573, https://doi.org/10.4314/ajtcam.v9i4.14.
[134] V. Steenkamp, E. Mathivha, M.C. Gouws, C.E.J. van Rensburg, Studies on antibacterial, antioxidant and fibroblast growth stimulation of wound healing remedies from South Africa, J. Ethnopharmacol. 95 (2004) 353–357, https://doi.org/10.1016/j.jep.2004.08.020.
[135] A.J. Josiah, S.K. Pillai, W. Cordier, M. Nell, D. Twilley, N. Lall, S.S. Ray, Cannabidiol-mediated green synthesis, characterization, and cytotoxicity of metal nanoparticles in human keratinocyte cells, ACS Omega 6 (2021) 29078–29090, https://doi.org/10.1021/ACSOMEGA.1C04303/ASSET/IMAGES/MEDIUM/AO1C04303_M001.GIF.
[136] M.E. Lediga, T.S. Malatjie, D.K. Olivier, D.T. Ndinteh, S.F. van Vuuren, Biosynthesis and characterisation of antimicrobial silver nanoparticles from a selection of fever-reducing medicinal plants of South Africa, South Afr. J. Bot. 119 (2018) 172–180, https://doi.org/10.1016/j.sajb.2018.08.022.
[137] I.Z. Matić, A. Mraković, Z. Rakočević, M. Stoiljković, V.B. Pavlović, T. Momić, Anticancer effect of novel luteolin capped gold nanoparticles selectively cytotoxic towards human cervical adenocarcinoma HeLa cells: an *in vitro* approach, J. Trace Elem. Med. Biol. 80 (2023) 127286, https://doi.org/10.1016/j.jtemb.2023.127286.
[138] R.G. Kudumela, L.J. McGaw, P. Masoko, Antibacterial interactions, anti-inflammatory and cytotoxic effects of four medicinal plant species, BMC Compl. Alternative Med. 18 (2018) 199, https://doi.org/10.1186/S12906-018-2264-Z.
[139] M.I. Fowler, K.Y.H.W. Yin, H.E. Humphries, J.E. Heckels, M. Christodoulides, Comparison of the inflammatory responses of human meningeal cells following challenge with *Neisseria lactamica* and with *Neisseria meningitidis*, Infect. Immun. 74 (2006) 6467–6478, https://doi.org/10.1128/IAI.00644-06.
[140] V.E. Mulaudzi, I.J. Adeosun, A.T. Adewumi, M.E.S. Soliman, S. Cosa, *Helichrysum populifolium* compounds inhibit MtrCDE efflux pump transport protein for the potential management of gonorrhoea infection, Int. J. Mol. Sci. 25 (2024) 13310, https://doi.org/10.3390/ijms252413310.
[141] H. Tseng, Y. Srikhanta, A.G. McEwan, M.P. Jennings, Accumulation of manganese in *Neisseria gonorrhoeae* correlates with resistance to oxidative killing by superoxide anion and is independent of superoxide dismutase activity, Mol. Microbiol. 40 (2001) 1175–1186, https://doi.org/10.1046/j.1365-2958.2001.02460.x.
[142] J.M. Griffiss, C.J. Lammel, J. Wang, N.P. Dekker, G.F. Brooks, *Neisseria gonorrhoeae* coordinately uses Pili and Opa to activate HEC-1-B cell microvilli, which causes engulfment of the gonococci, Infect. Immun. 67 (1999) 3469–3480, https://doi.org/10.1128/IAI.67.7.3469-3480.1999.
[143] L.M. Ball, A.K. Criss, Constitutively opa-expressing and opa-deficient *Neisseria gonorrhoeae* strains differentially stimulate and survive exposure to human neutrophils, J. Bacteriol. 195 (2013) 2982–2990, https://doi.org/10.1128/JB.00171-13.
[144] W. Pajerski, D. Ochonska, M. Brzychczy-Wloch, P. Indyka, M. Jarosz, M. Golda-Cepa, Z. Sojka, A. Kotarba, Attachment efficiency of gold nanoparticles by Gram-positive and Gram-negative bacterial strains governed by surface charges, J. Nano Res. 21 (2019) 186, https://doi.org/10.1007/s11051-019-4617-z.
[145] R.A. Jones, F. Ramirez-Bencomo, G. Whiting, M. Fang, H. Lavender, K. Kurzyp, A. Thistlethwaite, L. Stejskal, S. Rashmi, A.E. Jerse, A. Cehovin, J.P. Derrick, C. M. Tang, Tackling immunosuppression by *Neisseria gonorrhoeae* to facilitate vaccine design, PLoS Pathog. 20 (2024) e1012688, https://doi.org/10.1371/journal.ppat.1012688.
[146] V.D. Badwaik, L.M. Vangala, D.S. Pender, C.B. Willis, Z.P. Aguilar, M.S. Gonzalez, R. Paripelly, R. Dakshinamurthy, Size-dependent antimicrobial properties of sugar-encapsulated gold nanoparticles synthesized by a green method, Nanoscale Res. Lett. 7 (2012) 623, https://doi.org/10.1186/1556-276X-7-623.
[147] M.M. Saeed, E. Carthy, N. Dunne, D. Kinahan, Advances in nanoparticle synthesis assisted by microfluidics, Lab Chip 25 (2025) 3060–3093, https://doi.org/10.1039/D5LC00194C.
[148] M.G. Fuster, M.G. Montalbán, G. Carissimi, B. Lima, G.E. Feresin, M. Cano, J. J. Giner-Casares, J.J. López-Cascales, R.D. Enriz, G. Víllora, Antibacterial effect of chitosan–gold nanoparticles and computational modelling of the interaction between chitosan and a lipid bilayer model, Nanomaterials 10 (2020) 2340, https://doi.org/10.3390/nano10122340.
[149] C.R. Rogers, S. Dasari, A.K. Patlolla, P.B. Tchounwou, Physico-chemical characterization and assessment of cytotoxic and genotoxic effects of poly-ethylene-gycol coated and uncoated gold nanoparticles on human kidney (HK-2) cells, Austin J. Environ. Toxicol. 7 (2021) 1042.
[150] G. Li, H. Jiao, H. Yan, J. Wang, X. Wang, M. Ji, Establishment of a human CEACAM1 transgenic mouse model for the study of gonococcal infections, J. Microbiol. Methods 87 (2011) 350–354, https://doi.org/10.1016/j.mimet.2011.09.012.